Global Emissions and Abundances of Chemically and Radiatively Important Trace Gases from the AGAGE Network

Luke M. Western^{1,2}, Matthew Rigby¹, Jens Mühle³, Paul B. Krummel⁴, Chris R. Lunder⁵, Simon O'Doherty¹, Stefan Reimann⁶, Martin K. Vollmer⁶, Dickon Young¹, Ben Adam¹, Paul J. Fraser⁴, Anita L. Ganesan⁷, Christina M. Harth³, Ove Hermansen⁵, Jooil Kim³, Ray L. Langenfelds⁴, Zoë M. Loh⁴, Blagoj Mitrevski⁴, Joseph R. Pitt¹, Peter K. Salameh⁸, Roland Schmidt³, Kieran Stanley¹, Ann R. Stavert⁴, Hsiang-Jui Wang⁹, Ray F. Weiss³, and Ronald G. Prinn²

Correspondence: Luke M. Western (lwestern@mit.edu)

Abstract. Measurements from the Advanced Global Atmospheric Gases Experiment (AGAGE) combined with a global 12-box model of the atmosphere have long been used to estimate global emissions and surface mean mole fraction trends of atmospheric trace gases. Here, we present annually updated estimates of these global emissions and mole fraction trends for 42 compounds measured by the AGAGE network, including chlorofluorocarbons, hydrochlorofluorocarbons, hydrofluorocarbons, perfluorocarbons, sulfur hexafluoride, nitrogen trifluoride, methane, nitrous oxide, and selected other compounds. The data sets are available at https://doi.org/10.5281/zenodo.15372480. We describe the methodology to derive global mole fraction and emissions trends, which includes the calculation of semihemispheric monthly mean mole fractions, the mechanics of the 12-box model and the inverse method that is used to estimate emissions from the observations and model. Finally, we present examples of the emissions and mole fraction datasets for the 42 compounds.

10 1 Introduction

Quantifying the global emissions of halogenated and other long-lived radiatively and chemically important trace gases is crucial for estimating their environmental impacts, such as ozone layer destruction, and for evaluating the progress of mitigation efforts. depletion of the stratospheric ozone layer, and contributions to radiative forcing. Chlorofluorocarbons (CFCs), halons, and the solvents carbon tetrachloride (CCl₄) and methyl chloroform (CH₃CCl₃) are trace gases that have been phased out for emissive use under the Montreal Protocol on Substances that Deplete the Ozone Layer. Emissions of these gases persist because they are still contained within appliances, foams, and other applications, produced before their phase out, and continue to leak

¹School of Chemistry, University of Bristol, Bristol, UK

²Center for Sustainability Science and Strategy, Massachusetts Institute of Technology, Cambridge, MA, USA

³Scripps Institution of Oceanography, University of California San Diego, La Jolla, CA, USA

⁴CSIRO Environment, Aspendale, VIC, Australia

⁵NILU, Kjeller, Norway

⁶Empa, Laboratory for Air Pollution / Environmental Technology, Dübendorf, Switzerland

⁷School of Geographical Sciences, University of Bristol, Bristol, UK

⁸GC Soft Inc., Carlsbad, CA, USA

⁹School of Earth and Atmospheric Sciences, Georgia Institute of Technology, Atlanta, GA, USA

into the atmosphere. In some cases, production is ongoing because of their exempted production for chemical manufacture. Some of these substances remain in the atmosphere for years to centuries after they are emitted, owing to their long atmospheric lifetimes. Where non-ozone-depleting alternatives could not immediately be found, these gases were replaced by hydrochlorofluorocarbons (HCFCs), which are currently being phased out under the Montreal Protocol. HCFCs are in turn being replaced by hydrofluorocarbons (HFCs). While HFC do not deplete ozone, they have large global warming potentials, much like the ozone-depleting substances that they replaced. As a result, the production of HFCs is now being phased down under the Kigali Amendment to the Montreal Protocol. Chlorinated very short-lived substances (Cl-VSLS), with atmospheric lifetimes less than around six months, and some halomethanes, with both natural and anthropogenic sources, are not controlled under the Montreal Protocol and may present a threat to ozone layer recovery. Collectively, the controlled and uncontrolled ozone-depleting substances are responsible for almost all of the anthropogenic chlorine and bromine input to the stratosphere. There are a number of non-ozone depleting fluorocarbons that have extremely large global warming potentials, such as perfluorocarbons (PFCs), sulfur hexafluoride (SF₆) and nitrogen trifluoride (NF₃), and are almost entirely industrially produced. Halogenated substances, along with methane (CH_4) , which critically affects the oxidative capacity of the atmosphere, and nitrous oxide (N_2O) , which is also an ozone-depleting substance, are responsible for almost all the gaseous radiative forcing from anthropogenic sources beyond that of carbon 30 dioxide. As a result, monitoring of these gases is crucial to understand the state of the atmosphere.

The Advanced Global Atmospheric Gases Experiment (AGAGE, Prinn et al., 2000, 2018) network publicly releases measurements of the dry-air mole fractions of 45 atmospheric compounds (Prinn et al., 2022). Measurements made through AGAGE and its predecessors (see Section 2) were initially used to derive atmospheric lifetimes of CFC-11, CFC-12 (Cunnold et al., 1983) and other trace gases, (e.g., Prinn et al., 1983a, 1995, 2005; Rigby et al., 2013; Thompson et al., 2024). However, the predominant use of AGAGE measurements currently is to estimate global emissions and mole fraction trends over time (Section 4). Here, we present global emissions and derived mole fraction trends for 42 trace gases (Table 1), inferred from AGAGE measurements and a 12-box model of the atmosphere (estimates are not provided for hydrogen, carbon monoxide and trichloroethene). We refer to these quantities as AGAGE-derived products, which are available at https://doi.org/10.5281/zenodo.15372480 (Western et al., 2025). The primary purpose of this article is to describe the methodology underpinning these AGAGE-derived products.

Global emissions and mole fraction trends are derived using AGAGE measurements coupled with a two-dimensional 12-box model of the atmosphere (Cunnold et al., 1983, 1994; Rigby et al., 2013). This is in contrast to inventory methods, or bottom-up methods, using activity data and emission factors, which can quantify expected emissions. The estimated emissions presented here, also known as top-down emissions, are inferred from measured mole fraction. The modelled global and semi-hemispheric semihemispheric mole fractions presented (see Section 5) are also inferred using measurements. The reason for inferring the mole fractions, rather than directly using the measurements themselves, is primarily so that mole fractions can be inferred during times where no measurements are available, e.g., due to instrument downtime.

AGAGE-derived products of ozone-depleting substances (ODSs) and greenhouse gases (GHGs) have been used in the Scientific Assessments of Ozone Depletion of the World Meteorological Organisation (WMO) (e.g., Ehhalt and Fraser, 1988; Laube and Tegtmeier, 2023; Liang and Rigby, 2023; Daniel and Reimann, 2023) and in the Assessment Reports of the Inter-

governmental Panel on Climate Change (e.g., IPCC et al., 1990; Gulev and Thorne, 2023). Emission estimates using AGAGE measurements have been published in many research articles. Some recent notable outputs are the identification of excess CFC-11 emissions in eastern China after its global production phaseout (Montzka et al., 2021; Rigby et al., 2019; Park et al., 2021), of discrepancies in reported abatement and estimated global and Chinese HFC-23 emissions (Stanley et al., 2020; Adam et al., 2024), of a rapid increase in unregulated global and Chinese chloroform emissions (Fang et al., 2019), and of increases in ODS emissions used as feedstock after their phase-out for dispersive uses (Lickley et al., 2021; Vollmer et al., 2018; Western et al., 2023). Emission estimates from the AGAGE network have exposed various unusual or rapidly increasing trends in ODSs (e.g., Vollmer et al., 2015c; Liang et al., 2016; Vollmer et al., 2016; Simmonds et al., 2017; Vollmer et al., 2018; An et al., 2021; Western et al., 2022; An et al., 2023) and halogenated GHGs (Mühle et al., 2009; Miller et al., 2014; Simmonds et al., 2016; Fortems-Cheiney et al., 2015; Simmonds et al., 2014; Lunt et al., 2022). AGAGE measurements have also been used to identify several compounds in the atmosphere for the first time and to quantify their associated emissions (e.g., ?Mühle et al., 2009; Schoenenberger et al., 2015; Vollmer et al., 2015a, b, 2019, 2021)(e.g., Weiss et al., 2008; Mühle et al., 2009; S

We describe the AGAGE measurements used to derive the derived products in Section 2, the AGAGE 12-box model in Section 3, and the inverse framework in Section 4. A brief description of the contents of the AGAGE derived products is provided in Section 5. The atmospheric budgets derived from the products are then presented in Section 6. Finally, limitations are outlined in Section 7 and a brief summary is given in Section 8.

70 2 Measurements

65

80

The AGAGE network and its two predecessors have measured been measuring the atmospheric abundance of trace gases since 1978 (Atmospheric Lifetime Experiment, ALE: 1978–1981; Global Atmospheric Gases Experiment, GAGE: 1982–1992; AGAGE: since 1993). AGAGE measurements are combined with the 12-box model and an inverse method to produce the derived products presented here. A complete description of the measurements made by the AGAGE network and its two predecessors is given by Prinn et al. (1983b), Prinn et al. (2000) and Prinn et al. (2018), including detailed descriptions of the measurement instruments and the calibration scales used for each trace gas. Here, we only summarise those measurements used as inputs to the 12-box model (Section 3), which are only from a subset of measurement sites, compounds and measurements made in the current network and its predecessors, with a focus on sites that frequently measure well-mixed background air throughout the year, that is, excluding sites that regularly measure highly polluted air masses.

The data sets described in Section 5 use measurements from five historic AGAGE stations and two newer AGAGE sites: Zeppelin (ZEP), Svalbard, Norway (78.9°N, 11.9°E; began 2001), Mace Head (MHD), Ireland (53.3°N, 9.9°W; began 1987), Jungfraujoch (JFJ), Switzerland (46.5°N, 8.0°E; began 2000), Trinidad Head (THD), California, USA (41.1°N, 124.2°W; began continuously in 1995), Ragged Point (RPB), Barbados (13.2°N, 59.4°W; began 1978), Cape Matatula (SMO), American Samoa (14.2°S, 170.6°W; began 1978), and at Kennaook/Cape Grim (CGO), Tasmania, Australia (40.7°S, 144.7°E; began

Table 1. Compounds measured by the AGAGE network for which emissions and atmospheric mole fraction trends are estimated

Common Name	Chemical Formula	Common Name	Chemical Formula
PFC-14	CF ₄	HCFC-124	CHCIFCF ₃
PFC-116	C_2F_6	HCFC-132b	$CH_2ClCClF_2$
PFC-218	C_3F_8	HCFC-133a	CH_2CICF_3
PFC-318	c-C ₄ F ₈	CFC-11	CCl_3F
Sulfur Hexafluoride	SF_6	CFC-12	CCl_2F_2
Sulfuryl Fluoride	SO_2F_2	CFC-13	$CClF_3$
Nitrogen Trifluoride	NF_3	CFC-113/a ¹	$C_2Cl_3F_3$
HFC-23	CHF_3	CFC-114/a ²	$C_2Cl_2F_4$
HFC-32	CH_2F_2	CFC-115	$CClF_2CF_3$
HFC-134a	CH_2FCF_3	Halon-1211	$CBrClF_2$
HFC-152a	CH_3CHF_2	Halon-1301	$CBrF_3$
HFC-125	CHF_2CF_3	Halon-2402	$CBrF_2CBrF_2$
HFC-143a	CH_3CF_3	Methyl Chloride	CH_3Cl
HFC-227ea	CF_3CHFCF_3	Methyl Bromide	$\mathrm{CH_{3}Br}$
HFC-236fa	$CF_3CH_2CF_3$	Dichloromethane	CH_2Cl_2
HFC-245fa	$CHF_2CH_2CF_3$	Chloroform	$CHCl_3$
HFC-365mfc	$CH_3CF_2CH_2CF_3$	Carbon Tetrachloride	CCl_4
HFC-43-10mee	$CF_3(CHF)_2CF_2CF_3$	Methyl Chloroform	CH_3CCl_3
HCFC-22	$CHClF_2$	Perchloroethylene (PCE)	CCl ₂ =CCl ₂
HCFC-141b	CH_3CCl_2F	Methane	CH_4
HCFC-142b	CH_3CClF_2	Nitrous Oxide	N_2O

¹ CFC-113/a is a composite of the isomers CFC-113 (CCIF₂CCl₂F) and CFC-113a (CCl₃CF₃). However, the contribution of each isomer to the total mole fraction is not yet well understood.

85 continuously in 1978). Figure 1 shows the location of these stations. The AGAGE network contains many more sites than the ones used here. The measurement sites that have been used have been selected due to their usefulness in measuring air that is less impacted by nearby pollution, and therefore more representative of background conditions, and their longevity of measurements.

The data sets presented here are primarily derived from in situ high-frequency measurements (Section 2.1). For a subset of substances, the in situ measurements are complemented by measurements of archived air samples (Section 2.2). Measurements from the ALE network from two sites – Adrigole (ADR), Ireland (52°N, 10°W) and Cape Meares (CMO), Oregon (45°N, 124°W°W) – are used for CFC-11, CFC-12, CFC-113/a, CCl₄ and CH₃CCl₃ before measurements from MHD and THD are

 $^{^2}$ CFC-114/a is a composite of the isomers CFC-114 (CClF $_2$ CClF $_2$) and CFC-114a (CCl $_2$ FCF $_3$). As footnote 1 .

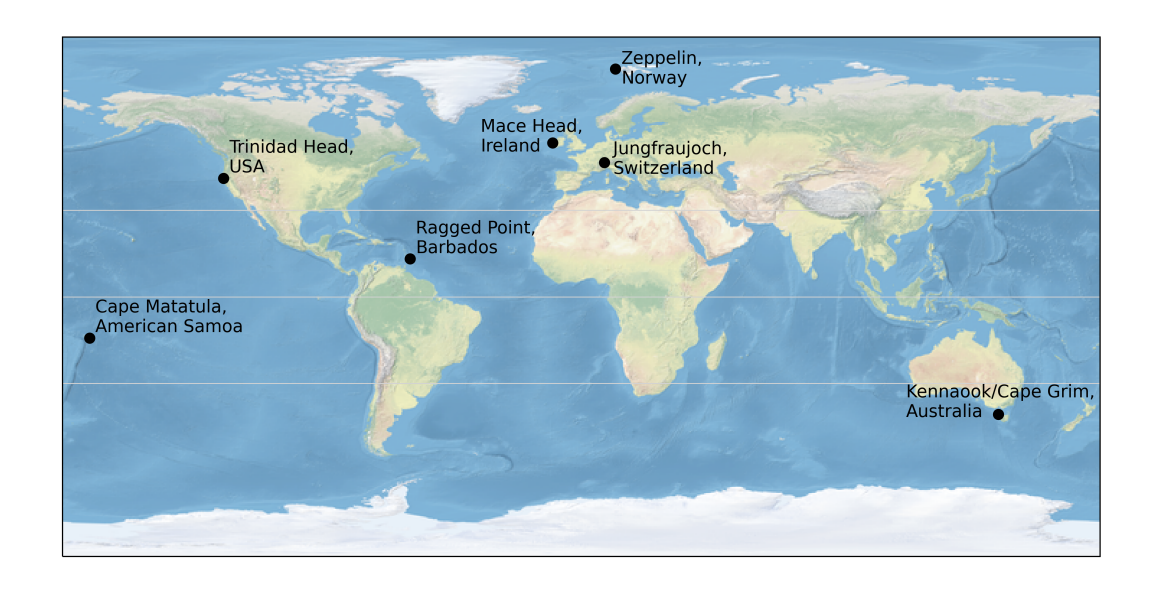


Figure 1. Locations of the AGAGE stations, from which measurements of dry-air mole fraction are currently used to derive the data sets using the 12-box model and an inverse method. Thin grey lines show the equator and $\frac{1}{2}$ and $\frac{1}{2}$ $\frac{1}{2}$

available. See Prinn et al. (1983b) for more information. Some publications have also used measurements of firn air, collected in Greenland and Antarctica, to derive emissions with the 12-box model (e.g., Trudinger et al., 2016; Vollmer et al., 2016, 2018), but the routinely published data sets presented here currently do not contain measurements made from firn air.

2.1 High-frequency measurements

100

Here, we describe the measurements used to derive global emissions and mole fraction trends. AGAGE in situ measurements of ODSs and GHGs have historically been made using multiple measurement instruments at each site. Measurements from Medusa gas chromatography mass spectrometry (GC-MS) systems (Miller et al., 2008; Arnold et al., 2012), deployed at each AGAGE site in the early to late 2000s and 2010s, are used to derive global emissions and mole fraction trends for most of the compounds listed in Table 1. Exceptions are CFC-11, CFC-12, CCl₄, and N₂O, for which measurements by the AGAGE gas chromatography 'multidetector' (GC-MD) systems at MHD, THD, RPB, SMO and CGO are preferentially used (in the

case of N_2O exclusively) due to higher measurement frequency and longer measurement records (see Prinn et al., 2000). These compounds are measured using electron capture detection (ECD) (Prinn et al., 2000). Sites that do not have a GC-MD instrument (JFJ and ZEP) were not used to estimate CFC-11, CCl₄, and N_2O mole fractions and emissions.

Prior to Medusa GC-MS measurements, some compounds had been measured on GC-MS adsorption—desorption systems (ADS), starting out with a prototype-ADS system at MHD in mid-1994, followed by ADS systems at MHD and CGO in late 1997 (see Simmonds et al., 1995; Prinn et al., 2000, for more information). GC-MS-ADS measurements also commenced at JFJ in 2000 (Reimann et al., 2004, 2008) and at ZEP in 2001 (Platt et al., 2022). Information about the compounds and time periods for which these GC-MS-ADS data are used to derive trends in emissions and mole fractions is contained in Prinn et al. (2025). All GC-MD, ADS, and Medusa measurements are reported on the calibration scales used by AGAGE, as detailed in Prinn et al. (2025).

Methane has been historically measured by AGAGE GC-MD systems (and its GAGE predecessor) using flame-ionization detection (FID), reported on the Tohuko 1987 scale maintained at SIO, but at some sites in recent years GC-MD CH₄ measurements have been replaced/superseded by cavity ring-down spectrometer (CRDS) instruments (Picarro) (see Prinn et al., 2018), reported on the NOAA-2004A scale (Dlugokencky et al., 2005). Extensive NOAA-AGAGE intercomparisons as well as AGAGE on-site instrument comparisons during instrument overlap have shown that the scale differences are negligible (NOAA/AGAGE ratio of 1.0001 ± 0.0007 , Prinn et al., 2018). Sites that do not have a GC-MD instrument (JFJ and ZEP) were not used for methane (even when CRDS measurements were available).

The typical repeatability of the measurements made by the GC-MS Medusa and GC-MD systems discussed here range from 0.05% for N₂O, 0.1% for CF₄ and CFC-12, 0.3-1% for most compounds, and up to 7% for HFC-236fa of the measured standard value. For CH₄, GC-MDs achieve 0.2% and CRDS systems achieve 0.02% (for more information see Prinn et al., 2018). The measurement repeatability is mainly compound and detector-dependent and is largely dominated by the atmospheric abundance of the compound but can also be negatively affected by site specific problems such as lab air contamination, lab temperature problems, trap temperature fluctuations, or MS filament problems.

The measurement data sets available from Prinn et al. (2025) provide details on the instruments used to measure each compound listed in Table 1, and for which period. The measurements are used in conjunction with the statistical AGAGE pollution algorithm to determine pollution free monthly mean baseline mole fractions, which are then used as input for the model and inversion to produce the data sets presented here. This method allows for the determination of monthly mean baseline mole fractions, as detailed in Section 2.3.

2.2 Archived air measurements

105

110

115

130

135

For several compounds, measurements of archived air samples are used to extend the in situ measurement record back into the past (available from Mühle et al., 2025). For the southern hemisphere Southern Hemisphere, air collection and archiving began in 1978 with the Cape Grim Air Archive (CGAA), where air samples were taken at CGO during clean air conditions with cryogenic methods and stored in stainless steel tanks (Fraser et al., 1991; Langenfelds et al., 1996), with the intention of reconstructing the historical composition of ambient air once suitable analytical instruments and calibration scales were

developed. Early measurements of the CGAA were performed on various instruments (summarized in Fraser et al., 2018), but here we focus on Medusa GC-MS measurement made in 2007 (e.g., Miller et al., 2010) and 2011 (e.g., Ivy et al., 2012), which were used in many subsequent studies (e.g., Mühle et al., 2009; O'Doherty et al., 2009; Rigby et al., 2010; O'Doherty et al., 2014). Later CGAA measurement made in 2016 (Vollmer et al., 2016) are currently not used here. These Medusa GC-MS measurements were mostly performed at the CSIRO Aspendale laboratory in Australia, but also at the Scripps Institution of Oceanography (SIO), in La Jolla, California USA. The frequency of available CGAA air samples differs, with one or two samples per year typically available before 1994, and up to nine samples available per year between 1994-1999, after which measurements of ongoing archived air samples are no longer used in this work. There is good agreement between the measurements at SIO and CSIRO of identical air samples and air samples with the same or similar fill dates.

To complement the CGAA, archived air samples from the Northern Hemisphere were gathered from several laboratories and mostly measured on Medusa GC-MS systems at SIO. Many of these tanks had been filled at THD or SIO, some at other northern hemispheric locations in the USA (such as Cape Meares in Oregon, Point Barrow in Alaska, and Niwot Ridge in Colorado) between 1973 and 2016 (Mühle et al., 2010, 2009). Unlike the CGAA, many of these samples were not originally intended for future atmospheric archive measurements and required more stringent quality control. For inert and/or volatile or very abundant compounds (such as CF₄, SF₆, NF₃, many HFCs and HCFCs) the resulting measurements were well-suited to reconstruct historic northern hemispheric abundances. Measurements of other compounds (e.g., several minor CFCs, H-2402, HCFC-124, HFC-43-10mee, PFC-218) produced some anomalous data points during data processing, which resulted in less certain northern hemispheric historic abundances for these compounds. Some archived air samples from the northern hemisphere were also measured at CSIRO (Arnold et al., 2012; Ivy et al., 2012; Mühle et al., 2010, 2009), again generally confirming that measurements from the instruments at SIO and CSIRO can be combined.

Table 2 shows the compounds that use archived air measurements in their emissions estimates. The references in Table 2 are the first publications in which archived air was used to derive emissions, and subsequent relevant publications.

2.3 Derivation of baseline mole fractions

150

155

Derived global emissions and mole fraction trends are inferred from monthly mean 'baseline' mole fractions for each measurement site in Section 2. A baseline measurement is when the sampled air is well mixed within the air parcel and is not influenced by nearby pollution sources. These monthly mean baseline mole fractions are fed into the inversion framework described in Section 4.

Here, monthly mean baseline measurements are derived using a statistical algorithm (O'Doherty et al., 2001). The algorithm identifies measurements that are considered as baseline by taking the following steps.

1. For a given day, fit a second-order polynomial to the daily minima of measurements over a 121-day window centred on that day (i.e. using 60 days before and after). Subtract the fitted polynomial from all measurements within the window, to detrend the measurements, and calculate the median of these detrended data. Calculate the root mean square error

Table 2. Relevant publications of compounds that have used archived air measurements, alongside high frequency measurements made by AGAGE, to quantify emissions estimates.

Compounds	Reference
CF ₄	Mühle et al. (2010); Trudinger et al. (2016)
C_2F_6	Mühle et al. (2010); Trudinger et al. (2016)
C_3F_8	Mühle et al. (2010); Trudinger et al. (2016)
c-C ₄ F ₈	Mühle et al. (2019)
SF_6	Rigby et al. (2010); Simmonds et al. (2020)
NF_3	Arnold et al. (2013)
$\mathrm{SO}_2\mathrm{F}_2$	Mühle et al. (2009)
HFC-23	Miller et al. (2010); Simmonds et al. (2018); Stanley et al. (2020)
HFC-32	O'Doherty et al. (2014)
HFC-125	O'Doherty et al. (2009)
HFC-134a	O'Doherty et al. (2004); Rigby et al. (2014)
HFC-143a	O'Doherty et al. (2014)
HFC-152a	Simmonds et al. (2016)
HFC-227ea	Vollmer et al. (2011)
HFC-236fa	Vollmer et al. (2011)
HFC-245fa	Vollmer et al. (2011)
HFC-365mfc	Vollmer et al. (2011)
HFC-43-10mee	Arnold et al. (2014)
HCFC-22	O'Doherty et al. (2004); Saikawa et al. (2012); Western et al. (2024b)
HCFC-141b	O'Doherty et al. (2004); Simmonds et al. (2017); Western et al. (2022)
HCFC-142b	O'Doherty et al. (2004); Simmonds et al. (2017); Rigby et al. (2014); Western et al. (2024b)
CFC-13	Vollmer et al. (2018)
CFC-115	Vollmer et al. (2018)
CFC-113/a	Rigby et al. (2014)
CFC-114/a	Vollmer et al. (2018)
H-1211	Vollmer et al. (2016)
H-1301	Vollmer et al. (2016)
H-2402	Vollmer et al. (2016)

(RMSE) using only the detrended values that fall below this median value. Classify measurements on the given day as baseline if they are within three times the RMSE of the median. Compute this step as a moving window across all days.

- 2. Repeat step 1 using the resultant tentative baseline measurements, with initial pollution events removed, from the first iteration of Step 1. Additionally, during this step, label measurements that fall within two to three times the new RMSE as 'possibly polluted' measurements.
- 3. Remove the 'possibly polluted' measurements if the following or preceding measurement is also labelled as a polluted measurement (i.e., greater than three times the RMSE) following Step 2.
- 4. The mean of the remaining baseline measurements for each calendar month is taken as the monthly mean baseline for a given measurement site.

3 AGAGE 12-box model

175

AGAGE measurements are combined with a 12-box model and an inverse method to produce the derived products presented

here. The AGAGE 12-box model is a two-dimensional model that simulates transport of long-lived trace species in the zonal
mean atmosphere (i.e., with no longitudinal component). Each trace gas is assumed to be uniformly mixed within each box.

The current AGAGE 12-box model has evolved from the 9-box model originally described in Cunnold et al. (1983), which was
later expanded to 12 boxes (Cunnold et al., 1994). Several subsequent publications have recoded this original model (Rigby
et al., 2013), updated transport parameters or losses (e.g., Rigby et al., 2008), or developed a model adjoint (Thompson et al.,
2018). The 12-box model is divided into latitudinal semi-hemispheres at the equator and 30 °N and 30 °S, and vertically at 500
and 200 hPa (with the surface at 1000 hPa), approximating boxes bounded at the planetary boundary layer and tropopause. See
Figure 2 for a schematic representation. The air masses of the four boxes are equal at each vertical level. The 12-box model is
governed by source, transport and loss processes, which are described in the remainder of this section.

3.1 Transport

Dynamic transport in the 12-box model is represented through a parameterisation of advection and diffusion between the boxes. The change in the mass mixing ratio in surface boxes (j = 0, 1, 2, 3), χ_j , over time is given by the equation

$$\frac{d\chi_{j}}{dt} = -\mathbf{1}_{j>0}(j) \left(V_{j-1,j} \bar{\chi}_{j-1,j} + \frac{(\Delta \chi)_{j,j-1}}{t_{j,j-1}} \right) - \mathbf{1}_{j<3}(j) \left(V_{j+1,j} \bar{\chi}_{j+1,j} + \frac{(\Delta \chi)_{j,j+1}}{t_{j,j+1}} \right) - \left(V_{j+4,j} \bar{\chi}_{j+4,j} + \frac{(\Delta \chi)_{j,j+4}}{t_{i,j+4}} \right) - L_{j} + \frac{E_{j}}{M_{j}}, \tag{1}$$

where $V_{i,k}$ is an inverse time constant representing the mean meridional transport between boxes i and k, $t_{i,j}^{-1}$ is the rate of eddy diffusion, E_j is the emissions into box j, the losses are defined collectively by L_j , and M_j is the total mass of air in box j. Other mathematical descriptors are

$$\bar{\chi}_{i,k} = \frac{1}{2}(\chi_i + \chi_k),\tag{2}$$

$$(\Delta \chi)_{i,k} = \chi_i - \chi_k,\tag{3}$$

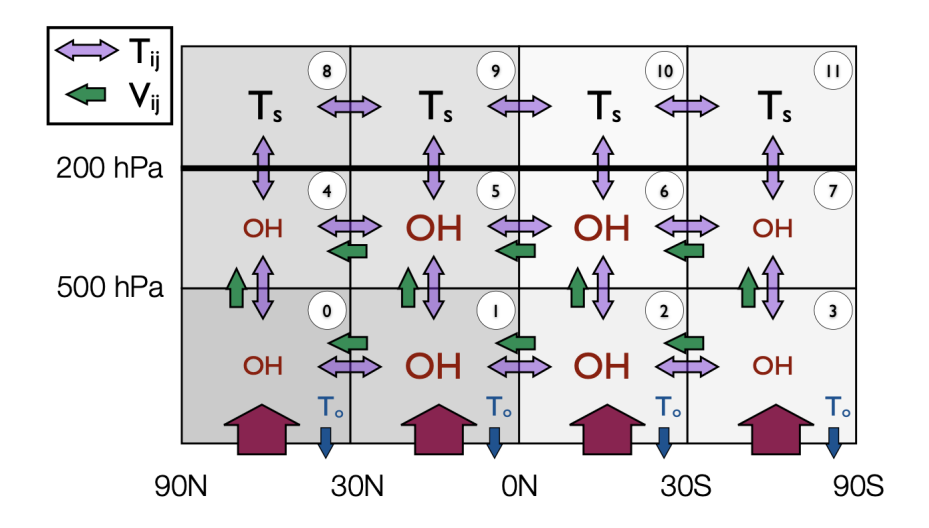


Figure 2. A schematic of the 12-box model taken from Rigby et al. (2013). The purple two-headed arrows between boxes indicate the eddy diffusion timescales and the green arrows the advection rates, which are shown in Table 3. The red arrows represent emissions into the model. Blue arrows, labelled with T_o , represent loss processes due to ocean and soil uptake. Boxes labelled with OH show where troposphoric loss due to reaction with the hydroxyl radical occurs. Boxes labelled T_s show where stratospheric loss occurs. The indices used to label each box are shown in the white circles. For methane, there is an additional loss field for the chlorine radical. For some species, such as halons, a first order loss is also assumed in the tropospheric boxes, parameterising tropospheric photolysis.

and the indicator function, which is defined where

200
$$\mathbf{1}_A(j) = \begin{cases} 1 & \text{if } A \text{ is true} \\ 0 & \text{otherwise.} \end{cases}$$
 (4)

For tropospheric boxes (j = 4, 5, 6, 7), the mass mixing ratio is given by

$$\frac{d\chi_{j}}{dt} = -\mathbf{1}_{j>4}(j) \left(\frac{5}{3} V_{j-1,j} \bar{\chi}_{j-1,j} + \frac{(\Delta \chi)_{j,j-1}}{t_{j,j-1}} \right) - \mathbf{1}_{j<7}(j) \left(\frac{5}{3} V_{j+1,j} \bar{\chi}_{j+1,j} + \frac{(\Delta \chi)_{j,j+1}}{t_{j,j+1}} \right) - \left(\frac{5}{3} V_{j-4,j} \bar{\chi}_{j-4,j} + \frac{5}{3} \frac{(\Delta \chi)_{j,j-4}}{t_{j,j-4}} \right) - \frac{(\Delta \chi)_{j,j+4}}{t_{j,j+4}} - L_{j},$$
(5)

and finally for the stratospheric boxes (j = 8, 9, 10, 11),

$$\frac{d\chi_j}{dt} = -\mathbf{1}_{j>8}(j) \frac{(\Delta\chi)_{j,j-1}}{t_{j,j-1}} - \mathbf{1}_{j<11}(j) \frac{(\Delta\chi)_{j,j+1}}{t_{j,j+1}} - \frac{3}{2} \frac{(\Delta\chi)_{j,j-4}}{t_{j,j-4}} - L_j.$$
(6)

Equations 1, 5 and 6 are solved using a Runge-Kutta (RK4) method (see e.g. Butcher, 1996) with a time step of 48 hours.

3.1.1 Transport coefficients

The mean meridional transport and eddy diffusion rates between the boxes vary seasonally but repeat annually. The advection parameters are taken from Cunnold et al. (1994), which were derived from a study by Newell et al. (1969). The original eddy diffusion terms estimated by Cunnold et al. (1983) have been adjusted in various ways in different studies. For example, Rigby et al. (2013) optimised the parameters simultaneously with CFC-11, CFC-12 and CFC-113 and CH₃CCl₃ lifetimes using AGAGE observations of those species, and Rigby et al. (2008) attempted to account for some inter-annual variability in transport by scaling inter-hemispheric exchange rates as a function of climate indices such as the Southern Oscillation Index. Here, we use the parameterisation that has been used in recent studies (e.g., Laube and Tegtmeier, 2023; Liang and Rigby, 2023) in which interannually repeating eddy diffusion parameters were derived based on simulations of an inert tracer in the MOZART three-dimensional model (Emmons et al., 2010). MOZART was run using NCEP/NCAR reanalyses for SF₆ for the years 2007 - 2009, as described in Rigby et al. (2011b). The box model mole fractions were compared to zonal mean mole fractions output from MOZART averaged over regions of the atmosphere chosen to be approximately representative of the mass-weighted centre of each box (45°- 80° for the extratropical boxes and 10° - 20° in the tropical boxes, and 1000 - 1000 hPa, 1000 - 1000 hPa, and 1000 - 1000 hPa in the vertical). These seasonal advection and eddy diffusion parameters are summarised in Table 3. The temperature in each box, which is used to calculate OH losses, is applied monthly, but is inter-annually repeating and is taken from the 1990-2010 mean from the NCEP/NCAR reanalysis (Kalnay et al., 1996).

3.2 Sinks and loss processes

215

220

230

235

The 12-box model has various loss processes, depending on the compound and box, which are summarised in Table 4. Where target lifetimes in the literature are given as a range, the median (with respect to the inverse lifetime, or loss frequency) is used. Compounds with total atmospheric lifetimes greater than 10,000 years are considered to have no atmospheric sink.

Losses due to the reaction with the hydroxyl radical (OH), for compounds with non-negligible OH losses, are calculated in the tropospheric boxes (boxes 0-70-7, see Figure 2). The concentrations of OH (taken from Spivakovsky et al., 2000) are seasonally varying but annually repeating and the OH field is adjusted so that the model mole fraction simulation of CH₃CCl₃, whose loss is dominated by OH, is consistent with AGAGE observations (using an approach similar to Rigby et al., 2013, but for inter-annually repeating, rather than inter-annually varying OH). All compounds are passive with respect to the OH loss, meaning that there is no loss of OH due to the sink process. Losses due to OH are computed using a first-order rate constant, using the Arrhenius equation and the temperature fields from Section 3.1.1. The Arrhenius factor and molar activation energy for each compound are taken from Burkholder et al. (2020). Where the OH sink is thought to be negligible and is not reported, a default Arrhenius factor of 1×10^{-30} and E/R factor of 1600 is assumed.

Losses in the stratosphere (boxes 8-11-8-11 in Figure 2), due to reaction with oxygen radicals, stratospheric OH and photolysis are calculated using a single first-order loss frequency that accounts for the overall loss due to these processes. Lyman- α photolysis is treated as a loss in the stratospheric boxes in the model, even though this sink is a mesospheric loss process. A suitable first-order rate constant for stratospheric losses for each compound is found by optimisation, such that the steady-state

Table 3. Transport parameters between boxes. Eddy diffusion parameters are available for transport between all boxes. Advection does not occur in the stratospheric boxes. Advection timescales are mass conserving.

Parameter	Box i	Box j	January-March January-March	April-June April-June	July-September July-September	October-De
	0	1	116	116	261	
	1	2	495	712	363	
	2	3	167	167	116	
	4	5	29	35	85	
	5	6	124	178	124	
	6	7	52	42	29	
	4	0	38	38	38	
Eddy diffusion, t_{ij}^{-1}	5	1	38	38	38	
(days)	6	2	38	38	38	
	7	3	38	38	38	
	8	4	1260	1260	1260	
	9	5	1260	1260	1260	
	10	6	1260	1260	1260	
	11	7	1260	1260	1260	
	8	9	100	100	100	
	9	10	100	100	100	
	10	11	100	100	100	
	0	1	-1506	581	1882	
	1	2	-69	-376	50	
	2	3	1506	1075	753	
	4	5	1506	-581	-1882	
Advection, V_{ij}	5	6	69	376	-50	
$(days^{-1})$	6	7	-1506	-1075	-753	
	4	0	-1506	581	1882	
	5	1	-72	-228	52	
	6	2	65	279	-54	
	7	3	-1202	-1087	-804	

stratospheric lifetime equals that in Burkholder and Hodnebrog (2023). An exception is the stratospheric lifetime of methane, which is taken from Myhre et al. (2014). Initial stratospheric losses are distributed latitudinally and temporally following Golombek and Prinn (1986), and these values are adjusted by a single factor in the optimisation, such that the relative temporal and spatial gradients are not altered. Target stratospheric steady state lifetimes are summarised in Table 4.

Compounds with sink processes due to ocean and/or soil uptake have losses in the lowest layer boxes (0-3-0-3 in Figure 2). In a similar manner to the stratospheric losses, ocean and soil losses are treated together as a single loss process. These losses are computed as a first-order loss, where the first order rate constant is optimised to give the steady-state target lifetime of the total soil and ocean loss (Burkholder et al., 2020; Yvon-Lewis and Butler, 2002).

245

250

For methane, loss from reaction with the chlorine radical is included in the model. The chlorine distribution is taken from Sherwen et al. (2016). First order rate constants are calculated using the Arrhenius equation (Burkholder and Hodnebrog, 2023).

Tropospheric loss processes so far not addressed are present for some compounds, such as a non-negligible photolysis sink in the troposphere. These other tropospheric sinks are implemented in boxes 4-7-4-7 (Figure 2) using a first-order rate constant that is optimised in a similar way to that of the stratospheric and ocean/soil sinks, using a target tropospheric lifetime (Burkholder and Hodnebrog, 2023), considering the other loss processes present. The spatial and temporal gradient of this loss follows that of loss from tropospheric OH.

Table 4: The loss coefficients for losses due to reaction with OH and the target lifetimes for loss process in the stratosphere, due to soil/ocean uptake and tropospheric losses other than OH. Losses due to OH are taken from Burkholder et al. (2020) and target lifetimes are taken from Burkholder and Hodnebrog (2023), where available. The stratospheric lifetime of methane is taken from Myhre et al. (2014). OH_A is the Arrhenius factor and $OH_{E/R}$ is the molar activation energy. Citations for these values are provided in the text.

Compound	OH_A	$\mathrm{OH}_{E/R}$	OH tropospheric lifetime (years)	Stratospheric lifetime (years)	Non-OH tropospheric lifetime (years)	Soil/ocean lifetime (years)
CF ₄	1.00×10^{-30}	$\frac{OH_{E/R}}{1600}$	The three type and the type and type and the	50000	meanic (years)	metime (years)
C_{14} $C_{2}F_{6}$	1.00×10^{-30}	1600		10000		
$C_2\Gamma_6$ C_3F_8	1.00×10^{-30}	1600		2600		
	1.00×10^{-30}	1600		3200		
<i>c</i> -C ₄ F ₈						
CFC-11	1.00×10^{-11}	9700		55		
CFC-12	1.00×10^{-11}	11900		103		
CFC-13	1.00×10^{-30}	1600		640		
CFC-113	1.00×10^{-11}	6200		94.5		
CFC-114	1.00×10^{-11}	6200		191		
CFC-115	1.00×10^{-11}	6200		664		
HCFC-22	9.20×10^{-13}	1560	12.6	120		1174
HCFC-124	7.10×10^{-13}	1300	6.3	105		1855
HCFC-132b	3.60×10^{-12}	1600	3.8	57.5		
HCFC-133a	9.40×10^{-13}	1300	4.8	82.6		
HCFC-141b	1.25×10^{-12}	1600	10.4	49.4		9190

Compound	OH_A	$\mathrm{OH}_{E/R}$	OH tropospheric lifetime (years)	Stratospheric lifetime (years)	Non-OH tropospheric lifetime (years)	Soil/ocean lifetime (years)
HCFC-142b	1.30×10^{-12}	1770	19.3	148		122200
CCl_4	1.00×10^{-11}	6200		44		93
$\mathrm{CH_{2}Cl_{2}}$	1.92×10^{-12}	880	0.5			<u>4211</u>
CH_3CCl_3	1.64×10^{-12}	1520	5.9	38		94
CH_3Cl	1.96×10^{-12}	1200	1.5	30.4		3.11
$CHCl_3$	2.20×10^{-12}	920	0.5			
CCl ₂ =CCl ₂	4.70×10^{-12}	990	0.4			
CH_4	2.45×10^{-12}	1775	10.4	150		
H-1211	1.00×10^{-12}	3500		41	26.24	
H-1301	1.00×10^{-12}	3600		73.5	3528	
H-2402	1.00×10^{-12}	3600		41	88.3	
$\mathrm{CH_{3}Br}$	1.42×10^{-12}	1150	1.7	26.3		1.61
HFC-23	6.10×10^{-13}	2260	248.8	3636		
HFC-32	1.70×10^{-12}	1500	5.5	146		
HFC-125	5.16×10^{-13}	1670	34.1	665		10650
HFC-134a	1.03×10^{-12}	1620	14.2	313		5909
HFC-143a	1.07×10^{-12}	2000	<u>54.9</u>	548		
HFC-152a	8.70×10^{-13}	975	1.5	44.3		1958
HFC-227ea	4.80×10^{-13}	1680	38.0	754		
HFC-236fa	1.45×10^{-12}	2500	247.0	136		
HFC-245fa	6.10×10^{-13}	1330	8.2	153.8		
HFC-365mfc	1.80×10^{-12}	1660	9.4	188		
HFC-43-10mee	5.20×10^{-13}	1500	18.1	360		
N_2O	1.00×10^{-30}	1600		109		
NF_3	1.00×10^{-30}	1600		740		
SF_6	1.00×10^{-30}	1600		1065		
SO_2F_2	1.00×10^{-30}	1600		630		40

255 4 Inverse method

The emission and global mole fraction trends for the compounds listed in Table 1 are derived using an inverse modelling framework. The approach relies on the measurements described in Section 2and an a priori set of emissions estimates, and a priori emissions estimates, to inform an estimate of emissions and mole fraction trends using Bayesian inference (Section 4.2).

This section describes the statistical framework to derive these estimates, the treatment of errors and uncertainties, and the a priori emissions used.

4.1 Statistical framework

260

265

275

280

285

290

The inverse framework here generally follows that of Rigby et al. (2011a, 2014). Emissions are derived based on the comparison of simulated mole fractions in the surface boxes and monthly background mean AGAGE observations. The monthly mean mole fraction in each box is calculated as the mean of the monthly mean mole fractions from all available measurement sites located in that box. We define \mathbf{x} as the deviation (in Gg yr⁻¹) from an a priori estimate of emissions taken from available bottom-up estimates of global emissions in the literature, \mathbf{x}_a (see Section 4.2). The a priori emissions estimate is the best independent estimate of emissions in the absence of information from atmospheric measurement. The corresponding observation \mathbf{y} is the deviation of the measured mole fractions from the modelled mole fraction using these a priori emissions. The relationship between the difference in emissions and surface mole fraction from the a priori estimate is

$$\mathbf{y} = \mathbf{H}\mathbf{x} + \epsilon, \tag{7}$$

where \mathbf{H} is a sensitivity matrix relating emissions to surface mole fractions and ϵ is a stochastic error, resulting from error in the mole fraction measurements. The vector \mathbf{x} is derived either monthly, seasonally or annually for each box, depending on the compound in question (see Supplementary Table S1 for this information). The sensitivity matrix \mathbf{H} is derived using the linear relationship between emissions and surface mole fractions by running the model with base (a priori) emissions and again with perturbed emissions (+1 Gg) for each surface box for each time period defined in Supplementary Table S1. The sensitivity of the mole fraction to emissions is calculated until the end of the period where measurements are available. The surface mole fractions (deviation), \mathbf{y} , are baseline monthly means as detailed in Section 2.3.

An initial first guess at the initial conditions of the mole fraction in the 12 boxes of the model uses a nine-year spin-up period using the a priori emissions field. The initial conditions (and **H**) are recursively adjusted to approximate the measurements using the a priori emissions. Sensitivities (and derived emissions) begin three years before the earliest measurement. These initial three years account for model spin-up and are not included in the output data sets.

Under the Bayesian framework, we choose to place a prior constraint on the growth in emissions, rather than their absolute value (Rigby et al., 2011a). The growth matrix \mathbf{D} operates on the emissions \mathbf{x} , to produce an emissions growth value, which we constrain by the a priori emissions growth \mathbf{g} . The uncertainty in the a priori emissions growth is taken as a percentage of the maximum a priori emissions, and the percentages used are defined in Supplementary Table S1 for each compound, where no box will have a growth less than 1% of the maximum global growth. Uncertainty in this growth is assumed to be independent between boxes and time steps, which we contain in the matrix \mathbf{P} .

We separate the random and systematic errors due to the measurements and modelling. Only the random components are included in the statistical evaluation of x and are assumed to be uncorrelated between boxes and time steps. These random errors are contained in the matrix R. The diagonal is composed of the quadratic sum of the typical measurement error (given

in Supplementary Table S1) and the variability of the baseline mole fractions in that month (see Section 2.3). This latter term is assumed to be a measure of model error, by accounting for the magnitude of variability not accounted for in the model.

Under an assumption of a normal likelihood and prior probability, the resultant relationship for the probability of the emissions given the measurements (deviation) is,

$$-\ln P(\mathbf{x} \mid \mathbf{y}) \propto (\mathbf{y} - \mathbf{H}\mathbf{x})^T \mathbf{R}^{-1} (\mathbf{y} - \mathbf{H}\mathbf{x}) + (\mathbf{D}\mathbf{x} - \mathbf{g})^T \mathbf{P}^{-1} (\mathbf{D}\mathbf{x} - \mathbf{g}), \tag{8}$$

which, by completing the square, allows determination of the maximum a posteriori probability (MAP) estimate of emissions, $\hat{\mathbf{x}}$, using

$$\hat{\mathbf{x}} = \hat{\mathbf{P}}(\mathbf{H}^T \mathbf{R}^{-1} \mathbf{y} + \mathbf{D}^T \mathbf{P}^{-1} \mathbf{g}), \tag{9}$$

where

300
$$\hat{\mathbf{P}} = (\mathbf{H}^T \mathbf{R}^{-1} \mathbf{H} + \mathbf{D}^T \mathbf{P}^{-1} \mathbf{D})^{-1}, \tag{10}$$

and $\hat{\mathbf{P}}$ is the resultant posterior covariance matrix, representing the random error in the emissions estimate. The estimate $\hat{\mathbf{x}}$ is added to the initial a priori emissions to give the estimated total emissions. The posterior mean mole fractions are estimated using the relationship

$$\hat{\mathbf{y}} = \mathbf{H}\hat{\mathbf{x}} + \mathbf{H}\mathbf{x}_a. \tag{11}$$

Combined systematic and random uncertainties are derived through the random sampling of systematic uncertainties and the Cholesky decompostion of $\hat{\mathbf{P}}$. The systematic uncertainties are due to errors in the calibration, lifetime and transport. Calibration uncertainty is treated as a percentage offset, where the one standard deviation calibration uncertainties for each compound are defined in Supplementary Table S1. The systematic component of transport error is assumed to be 1 % of emissions for all substances (one standard deviation). Lifetime error variance is calculated as,

310
$$\sigma_x^2 = (B\sigma_{\perp})^2$$
, (12)

where B is the total atmospheric burden of the compound and $\sigma_{\frac{1}{\tau}}$ is the total inverse lifetime error (Ko et al., 2013) (see Rigby et al., 2014, for more information). The assumed lifetime uncertainty is shown in Supplementary Table S1 for each compound. The total uncertainty is then taken as the standard deviation from this ensemble.

4.2 A priori emissions

An initial set of estimates of the emissions for each compound has been compiled over time. These are from a variety of sources and can be found as supplementary data sets. Given the longevity of measurements made by the AGAGE network and their widespread use, there could be a lack of independence of the a priori emissions if taken from widely used emissions scenarios, which may have been, at least partly, informed by mole fraction measurements and/or emissions derived by AGAGE (e.g., Meinshausen et al., 2020). We have therefore strived, insofar as possible, to use independent a priori emissions estimates.

A priori emissions for CF₄, C₂F₆, C₃F₈, *c*-C₄F₈, HFC-23, HFC-32, HFC-125, HFC-134a, HFC-143a, HFC-152a, HFC-227ea, HFC-236fa, HFC-245fa, HFC-365mfc, HFC-43-10mee, HCFC-141b, HCFC-142b and SF₆ are taken from the gridded flux maps from the Emissions Database for Global Atmospheric Research (EDGAR) v8 (Crippa et al., 2023). These are annual emissions from 1970-20221970-2022, with the exception of C₃F₈, which spans 1975-20221975-2022. HFC-23 emissions prior to 1970 are taken from Miller et al. (2010). After 2022, emissions for all compounds are repeated using the values from 2022.

The EDGAR v8 inventory also includes NF₃ but its global emissions are erroneously small compared to other literature sources (e.g., Arnold et al., 2013; Liu et al., 2024). We instead use the PRIMAP-hist v2.6 national historical emissions time series for NF₃ (Gütschow et al., 2016, 2024). Emissions are quantified until 2023 in the database and repeated thereafter.

CFC-11, CFC-12 and CFC-113/a a priori emissions are the bottom-up estimates compiled in Rigby et al. (2013), which were informed by a variety of inventory compilations and forecasts (e.g., McCulloch et al., 2001, 2003). CH₃CCl₃ was compiled in a similar manner, but emissions have been repeated after 2015 until present. A priori estimates of CFC-114/a and CFC-115 were compiled from a variety of sources (see Vollmer et al., 2018, and its supplementary information). To the best of our knowledge, no comprehensive inventory of global emissions of CFC-13 exists, so we assume that the a priori emissions for CFC-13 are a seventh of those of CFC-115 (see the supplementary information of Vollmer et al. (2018) for the rationale behind this approximation, which is based on available ratios of production of the two compounds).

The prior emissions estimate for halons – Halon-1211, Halon-1301 and Halon-2402 – are taken from the bottom-up emissions published by Vollmer et al. (2016). These estimates were originally compiled by HTOC (2014) but the values were not made available.

335

340

The historic a priori estimates of CCl₄ emissions are based on information from industry on the production of CFCs (McCulloch, *personal communication*). Estimates since 2010 are taken from Sherry et al. (2018). The use of carbon tetrachloride as a feedstock for the production of CFCs was its major source of emissions prior to the phase out of the production of CFCs for dispersive uses. There are continued unexplained global emissions of carbon tetrachloride, which makes a comprehensive bottom-up inventory of its emissions difficult (Liang et al., 2016; Daniel and Reimann, 2023).

Little is known about the source of emissions of HCFC-132b and HCFC-133a (Fraser et al., 2014; Vollmer et al., 2015c, 2021).

These two substances are assumed a priori to have constant emissions, with an annual mean of 1 Gg yr⁻¹ with a small seasonal trend, following Vollmer et al. (2021). HCFC-22 a priori emissions are an extension of the bottom-up emissions derived by Miller et al. (1998), using the HCFC-22 production data from multiple sources (Miller et al., 2010). These emissions estimates extend through 2009, after which the emissions are assumed to remain constant. A bottom-up inventory of emissions for HCFC-124 was compiled for 1990-2001 and projected to 2015 under three scenarios (Ashford et al., 2004). We use Scenario 2, which envisaged improvements to reduce HCFC emissions over the policy at the time of compilation. Emissions are repeated after 2015.

PCE (CCl₂=CCl₂) a priori emissions are taken from Montzka and Reimann (2010), which was compiled from multiple sources (McCulloch et al., 1999; Keene et al., 1999; Simmonds et al., 2006). CH₂Cl₂, CHCl₃ and CH₃Cl estimates are based

on the emission estimates compiled in Xiao (2008) and methyl bromide in Yvon-Lewis and Butler (1997). Given the lack of a priori information about emissions of these gases, they are assumed to be constant in time.

The a priori estimates for SO_2F_2 were described in Mühle et al. (2009), which were compiled using information on the production of SO_2F_2 . Given the use of SO_2F_2 as a fumigant, it can be assumed that its emissions will be approximately equal to its production in a given year. Our prior emissions estimate for this compound was constant after 2007.

Emissions for N₂O are built from various sources. Anthropogenic emissions are from EDGARv8.0 for the years 1970-2022, and the 2022 emissions are repeated thereafter (Crippa et al., 2023). Ocean emissions are from the ECCO-Darwin model for the period 2009-2013 (Resplandy et al., 2024), and annually repeating before 2009 using the 2009 emissions and after 2013 using the 2013 emissions. Other natural emissions are from Saikawa et al. (2014) for 1990-2008 1990-2008, with annually repeating values using emissions from 1990 and 2008 before and after these dates. This estimate is within the range of bottom-up derived N₂O net flux (Tian et al., 2024).

Anthropogenic a priori emissions of CH₄ are taken from EDGAR v8.0 (Crippa et al., 2023), wetland emissions are taken from WetCHARTS v1.3.1 (Bloom et al., 2017), biomass burning from the Global Fire Emissions Database (GFED) (van der Werf et al., 2017), freshwater emissions from Stell et al. (2021), rice from Yan et al. (2009), and other natural sources from Fung et al. (1991); Ruppel and Kessler (2017). Years without estimates from a particular source are filled with the closest year of available data. The total emissions are within the uncertainty of other well-used bottom-up total flux estimates (e.g. Saunois et al., 2025).

4.3 Derived global mole fractions and growth rates

The presented mole fractions for each semihemisphere are those of the MAP estimate of the emissions, and their uncertainty, forward simulated through the 12-box model. The global annual mole fraction is the mean of the four surface-level boxes. The growth rates of the mole fraction are derived from $\hat{\mathbf{y}}$ (see Section 4.1) using backward differencing. These growth rates are then smoothed using a Kolmogorov–Zurbenko (KZ) filter (Yang and Zurbenko, 2010) with a window size of 9 and a filtering degree of 4. The uncertainties for the estimated mole fractions and their growth rates are derived from the Monte Carlo ensemble described in Section 4.1.

5 Published products

355

375

380

385

We aim to provide updated estimates of global missions and mole fraction trends annually, with a target time delay of approximately six months following the quality control of the atmospheric measurements by the AGAGE community. The release of data sets of specific substances may be withheld if the scientific integrity of the measurement of a specific substance is under question, e.g., due to emerging chromatographic interference, or if further insights into the data are required. Recent emission estimates (within the previous \sim 2 years) should be treated as preliminary as some of the underlying measurement data may not be fully vetted and/or calibration tanks may not have been returned from the measurement sites to the AGAGE central calibration laboratory for re-calibration.

For each substance, a number of derived products are provided. These summary data sets provided are as follows:

- Emissions:
 - Global annual emissions (with and without systematic uncertainties)
- Mole fraction:

400

405

410

- Global calendar year mean surface mole fraction (mid-year centred)
 - Global annual January-centred surface mole fraction
 - Semi-hemispheric Semihemispheric monthly mole fraction at each altitude level
 - Semi-hemispheric Semihemispheric monthly measured surface mole fraction
 - Surface mole fraction growth rate:
- **Global monthly mole fraction growth rate**
 - Semi-hemispheric Semihemispheric monthly mole fraction growth rate.

The data sets are provided as text files with comma-separated values (csv) and are available to download from Western et al. (2025). Each data set includes both the mean posterior estimate of the emissions/mole fraction (see Section 4) and its 1-standard deviation uncertainty. Annual emissions are provided including either random uncertainties or combined random and systematic uncertainties (see Section 4.1). These two uncertainty estimates are provided to aid the calculation of uncertainty in quantities that are, or are not, influenced by systematic uncertainties. The uncertainty in an emissions change between two years is not strongly influenced by systematic uncertainties of the type estimated here, whereas the uncertainty in the absolute emissions in a particular year is. For example, if an error in the measurement calibration scale for an inert compound causes a constant absolute offset across the whole measurement record, the derived emissions would also be offset by some near-constant value, yet the growth in emissions would remain unchanged. The annual and monthly quantities are centred around the corresponding calendar year or month, unless otherwise stated.

6 AGAGE derived global budgets

Here we give a summary of the budgets of non-CO₂ GHGs and ODSs derived from the AGAGE network through 2023 using the measurements from Prinn et al. (2025) and the methodology outlined above. We present these budgets separately for the long-lived halogenated gases that are primarily of synthetic anthropogenic origin in Section 6.1, and CH₄ and N₂O, whose fluxes have substantial non-anthropogenic components, in Section 6.2. Given the uncertain natural sources, short lifetime and uncertain impacts of very short-lived chlorinated substances (CH₂Cl₂, CHCl₃ and CCl₂=CCl₂), CH₃Cl and CH₃Br, we present these separately in Section 6.3. Emissions, global mole fractions, and their growth rates for each individual compound can be found in the supplementary information.

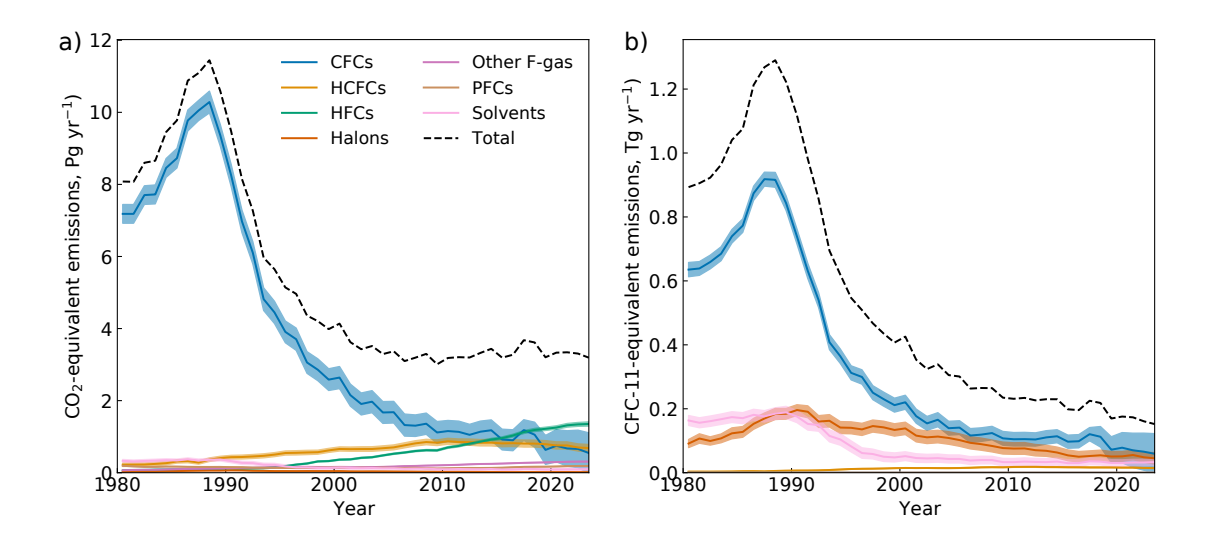


Figure 3. Emissions of synthetic greenhouse gases presented as the total, weighted in terms of their (a) global warming potential (CO₂-equivalent emissions) over a 100-year time horizon and (b) ozone-depleting potential (CFC-11-equivalent emissions). The category 'solvents' contains carbon tetrachloride and methyl chloroform, and the category 'other F-gases' contains SF₆, NF₃ and SO₂F₂.

415 6.1 Halogenated ozone-depleting substances and greenhouse gases

420

425

The annual global emissions of synthetic greenhouse gases are presented in Figure 3. We group compounds as CFCs, HCFCs, HFCs, Halons, 'other F-gases' (SF₆, NF₃ and SO₂F₂), PFCs and 'Solvents' (CCl₄ and CH₃CCl₃). These emissions are shown in terms of the direct climate warming potential of the emissions over a 100 year time horizon (GWP-100, CO2-eq) and their ozone depletion potential (ODP, CFC-11-eq) (Burkholder and Hodnebrog, 2023), respectively.

The total climate warming emissions from synthetic greenhouse gases were 3.2 ± 0.6 Pg CO₂-eq in 2023, and have remained relatively unchanged over the last 20 years of the record (Figure 3). There has been an overall reduction in CO₂-equivalent emissions due to reduction of CFC emissions since the 1990s. This reduction has been partially offset by a growth and recent decline in emissions of HCFCs (e.g., Western et al., 2024b), and the continuing growth of HFCs and, to a lesser extent, PFCs and other F-gases. It can reasonably be expected that the emissions of synthetic greenhouse gases will decrease in the coming years given the controls on HFCs under the Kigali Amendment to the Montreal Protocol and other commitments as part of the Paris Agreement and other climate policies (Velders et al., 2022; Daniel and Reimann, 2023).

The emissions of the ozone-depleting synthetic greenhouse gases (CFCs, HCFCs, halons and chlorinated solvents) were 152 ± 66 Gg CFC-11-eq in 2023. Emissions of these ozone-depleting substances are now at their lowest since measurement-derived emission records began, despite some small, but impactful, fluctuations in total emissions, meaning that this decline has not been entirely monotonic (see, e.g., Montzka et al., 2018, 2021).

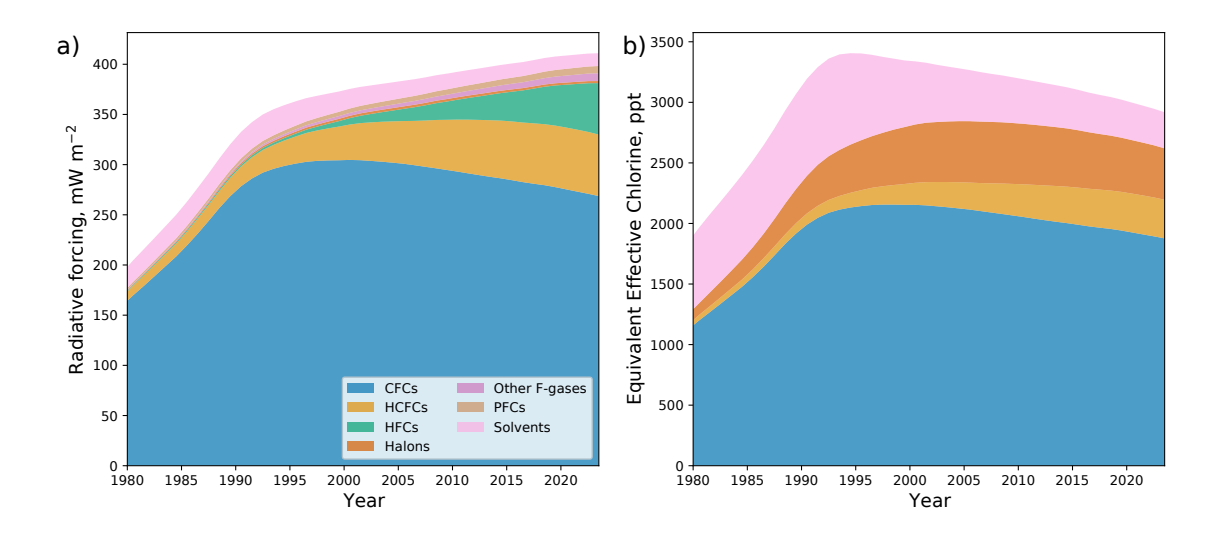


Figure 4. Global abundance of synthetic greenhouse gases in terms of (a) the direct radiative forcing and (b) equivalent tropospheric chlorine. The direct radiative forcing considers stratospheric adjustments to the instantaneous radiative forcing, and also the tropospheric adjustments for CFC-11 and CFC-12.

The global abundances of the synthetic greenhouse gases are shown in Figure 4, using the same compound groupings as Figure 3. The impact on climate is shown in terms of direct radiative forcing, which considers stratospheric adjustments to the instantaneous radiative forcing, and also tropospheric adjustments for CFC-11 and CFC-12 (Shine and Myhre, 2020; Hodnebrog et al., 2020; Burkholder and Hodnebrog, 2023). The impact on ozone depletion is shown in terms of equivalent effective chlorine (Montzka et al., 1996), which is the global mean surface chlorine mole fraction (number of chlorine atoms in a given species multiplied by its mole fraction).

The direct radiative forcing of synthetic greenhouse gases has increased since measurements of their atmospheric abundance began, reaching $411 + 5 \text{ mW m}^{-2}$ in 2023. Global abundances of CFCs, chlorinated solvents and HCFCs are now decreasing (Montzka et al., 1996; Western et al., 2024b), and are being offset by an increasing abundance of HFCs, PFCs (foremost CF₄) and other F-gases (foremost SF₆).

Conversely, the equivalent effective chlorine has declined since its peak in 1994, to 2920 ± 30 ppt in 2023. This is driven by the decreasing abundances of CFCs, halons and solvents (foremost CH₃CCl₃) in the atmosphere (Montzka et al., 1996) and also more recently by a fall in the abundance of HCFCs (Western et al., 2024b).

6.2 Methane and Nitrous Oxide

435

440

Figure 5 shows the global and semi-hemispheric semihemispheric mole fractions of methane and nitrous oxide, the growth rate of these mole fractions and the north-south inter-hemispheric difference. Figure 6 shows their global mean emissions.

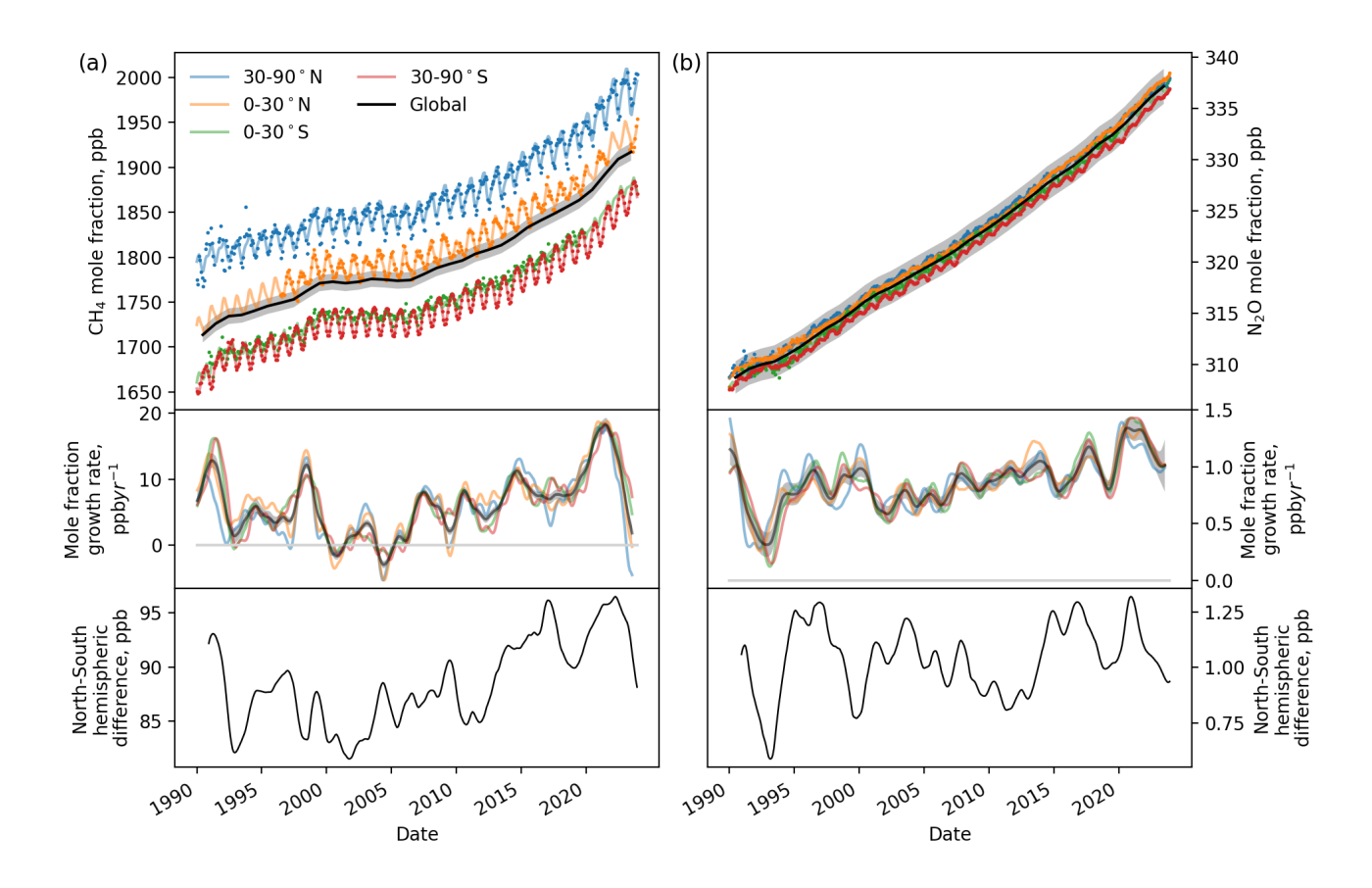


Figure 5. The global and semihemispheric mole fraction for (a) methane and (b) nitrous oxide (top panels), the growth rate in these mole fractions (middle panels) and the north-south interhemispheric difference (lower panels) for 1990-2023 1990-2023. Observed mole fractions are shown in the top panels by the small circles and fits to these observations are shown with lines. The black lines indicate global mean quantities with 1-sigma uncertainties shown by the grey shading.

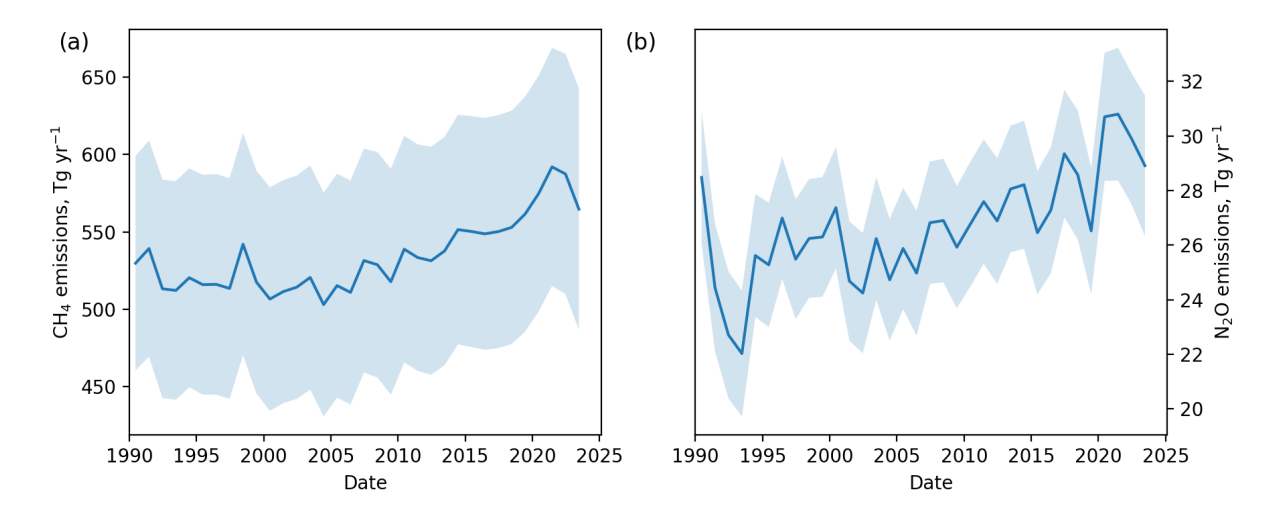


Figure 6. Global annual emissions of (a) methane and (b) nitrous oxide for 1990-2023 1990-2023. Shading indicated the 1 s.d. uncertainty due to measurement repeatability, model uncertainty, calibration scale uncertainty and lifetime uncertainty.

The global mean mole fraction of methane reached 1917 ± 10 ppb in 2023, following an accelerating rate of growth since a plateau in the global mole fraction during the mid-2000s (Rigby et al., 2008). This increase in the global mole fraction is coupled with an increase in the north-south interhemispheric difference. Global net emissions of methane in 2023 were 579 \pm 73 Tg yr⁻¹. In 2020 these emissions were 564 ± 78 Tg yr⁻¹, which falls within the range of top-down emissions derived for methane in multiple studies, of 608 [561-650] Tg (Saunois et al., 2024). The main drivers behind the increases and times of stagnation in direct methane emissions and the resulting global mole fraction are uncertain and may come from a mixture of natural and anthropogenic source and sink processes (Nisbet et al., 2016; Schaefer et al., 2016; Rigby et al., 2017; Turner et al., 2017; Worden et al., 2017; Jackson et al., 2020; Feng et al., 2023; Zhang et al., 2023).

The global mean mole fraction of nitrous oxide reached 337 \pm 2 ppb in 2023, following an increasing rate of growth since direct measurement records began. The north-south interhemispheric difference has shown substantially interannual variability but no obvious overall trend during this time. Global annual net emissions reached 29 \pm 3 Tg yr⁻¹ in 2023. In 2020 global net emissions were 31 \pm 2 Tg yr⁻¹, which is larger than the range of 26.7 (26.1-27.3) Tg yr⁻¹ (mean and range) for 2020 from four top-down approaches (Tian et al., 2024), but close to the estimate of 30.4 (29.7-31.6) Tg yr⁻¹ in Stell et al. (2022). The emissions in 2020 are within the range of bottom-up estimates of 29.1 (16.7-42.4) Tg yr⁻¹ presented in Tian et al. (2024).

6.3 Very short-lived chlorinated substances, methyl chloride and methyl bromide

455

460

Very short-lived substances (VSLSs) have total atmospheric lifetimes of less than around 6 months. Dichloromethane (CH_2Cl_2) and chloroform ($CHCl_3$) have natural as well as anthropogenic sources, although the natural emissions of CH_2Cl_2 are relatively minor (McCulloch, 2003; Simmonds et al., 2006). The atmospheric mole fraction of CH_2Cl_2 , and its emissions, have been

continuously increasing during the atmospheric record (Figure 7 and see, e.g., Trudinger et al. (2004)). Its global mean mole fraction has approximately doubled between 2008 and 2023, when it reached 41.5 ± 1.3 ppt, which has been driven mostly by increased emissions from China (An et al., 2021). Mole fraction and emissions of CHCl₃ have increased rapidly until 2015 (Fang et al., 2019), after which they have fallen to levels seen in the 2000s. Perchloroethylene (CCl₂=CCl₂) has only anthropogenic sources and its atmospheric abundance and emissions have been falling since the measurement record began.

Methyl chloride (CH₃Cl) has an atmospheric lifetime of 10-11 months. It has a mixture of natural and anthropogenic sources (Rhew et al., 2000). Its atmospheric mole fraction has remained fairly constant at around 550 ppt and its emissions at 4500-5000 Gg yr⁻¹ over the measurement record. Methyl bromide (CH₃Br) has an atmospheric lifetime of 9-10-9-10 months. It has a mixture of natural and anthropogenic (foremost fumigation) sources (Laube and Tegtmeier, 2023). Its production for all applications other than quarantine and pre-shipment purposes has been phased out under the Montreal Protocol, and its atmospheric mole fraction and emissions have been declining over the measurement record (Figure 7).

7 Limitations

470

475

490

495

Whilst the data sets presented here have been extremely useful for many studies charting the atmospheric and emissions history of these substances, users should be aware of their limitations. Failure to account for these limitations could lead to erroneous conclusions being drawn from the underlying AGAGE data.

The use of a box model of atmospheric transport to estimate emissions and mole fractions is associated with numerous potential issues. Emissions estimates on scales smaller than the model resolution are not possible. However, we also find that the coarse parameterisation of atmospheric transport precludes reliable semihemispheric emissions estimates, even at the model resolution. For that reason, we do not present semi-hemispheric semihemispheric emissions estimates, only semi-hemispheric semihemispheric mole fractions (which are better constrained by the measurements themselves). Furthermore, numerous studies have shown that the use of interannually repeating meteorology can lead to specious year-to-year fluctuations in global emissions due to the lack of influence from large-scale dynamical changes (e.g., Ray et al., 2020; Montzka et al., 2021). Due to the lack of interannually varying OH and other sinks, longer term trends in emissions and year-to-year differences may be misrepresented (e.g., Rigby et al., 2008, 2017; Turner et al., 2017; Naus et al., 2019).

Currently, emission estimates are only possible in the four lowest boxes. Therefore, emissions from aircraft or other airborne sources cannot be simulated. This includes in-atmosphere production of atmospheric breakdown products, for example, the proposed production of HFC-23 due to ozonolysis of some hydrofluoroolefins (HFOs) (McGillen et al., 2023). The lack of an explicit chemistry scheme would make any such processes difficult to include at present. Following the uptake of a trace gas by the ocean, there is the possibility that this current loss process instead becomes a source (Wang et al., 2021). This effect is neglected in the model as ocean/soil uptake is only a loss process, and should not impact the compounds of interest for the foreseeable future.

The isomers of some compounds are not currently separated using the instrumentation described in Section 2, as noted in Table 1. For example, the isomers CFC-113 and CFC-113a are not currently separated, and the reported mole fraction is

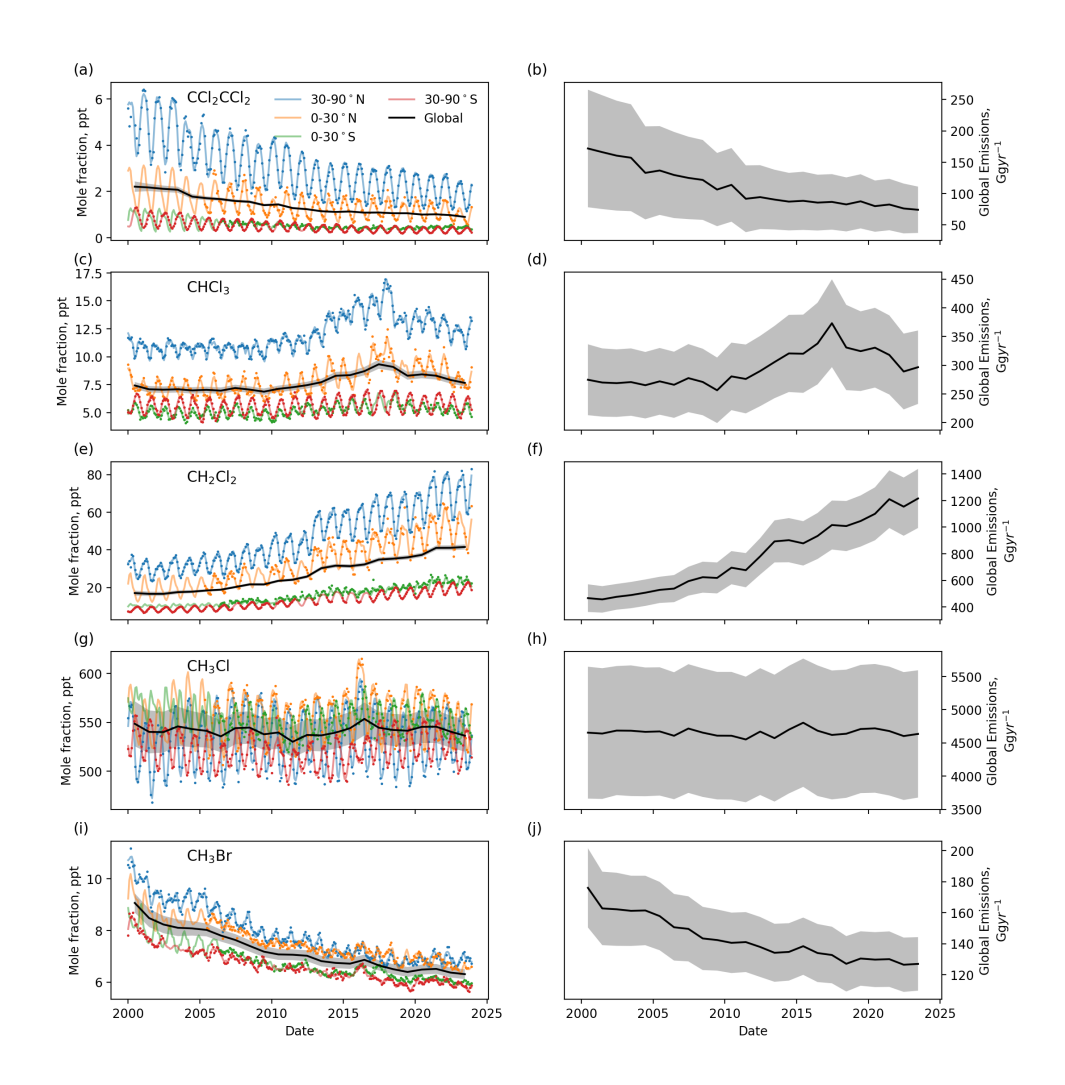


Figure 7. Semihemispheric and global mean mole fractions for (a) perchloroethylene, (c) chloroform, (e) dichloromethane, (g) methyl chloride and (i) methyl bromide. Circles show the observed semihemispheric mole fractions and the lines show the fits to these data. Their global emissions are shown in panels (b,d,f,h,j). Shading indicated the 1 s.d. uncertainty.

generally reported as a somewhat ill-defined combination of both isomers (Montzka et al., 2025). This issue has become more important in recent years because the more minor abundant isomer for some isomer pairs (e.g., CFC-113/a, CFC-114/a) has been increasing in the atmosphere (Western et al., 2023). Emissions and mole fraction trends for these individual isomers cannot be properly quantified at present.

The inverse method employed in this work, which constrains the emissions growth rate, is not strongly influenced by overall biases in the total magnitude of a priori emissions, compared to methods that constrain absolute emissions (Rigby et al., 2011a). However, the magnitude of the a priori growth uncertainty is informed by growth in the a priori emissions, or else chosen somewhat heuristically. Furthermore, spatial constraints are difficult to impose simultaneously with the growth constraint on emissions, as are non-negative emissions constraints. It would be preferable to employ an approach that allows physical limits to be applied to emissions and was less dependent on poorly understood uncertainties (e.g., Ganesan et al., 2014).

Since AGAGE measures trace gases at a frequency on the order of hours, a filter must be applied to provide estimates of baseline monthly mean mole fractions, which are used in combination with the box model (see Section 2.3). The current AGAGE statistical baseline method is simple and efficient to apply, but it can be unreliable, particularly at the beginning and end of the dataset, before and after prolonged periods of instrumental downtime, during periods of poor precision, for highly polluted species/sites, or for sites that are influences by monsoons. An alternative approach would use air histories to identify unpolluted periods and may be used in future versions (Manning et al., 2021).

Finally, our derived emissions estimates are sensitive to potential biases in the observations and model. Estimates are available for the uncertainty due to the assumed atmospheric lifetime and calibration scale, and these terms are included in our derived emissions estimates. However, for some compounds, particularly those with shorter lifetimes, unaccounted-for biases may exist because the network and model cannot resolve zonal gradients or meridional gradients within each box. For example, a difference between AGAGE and NOAA-derived dichloromethane emissions is thought to be partly due to differences in measurement locations in the Northern Hemisphere tropics between the two networks, as well as a large ($\sim 10\%$) difference in calibration scales (Carpenter and Reimann, 2014).

8 Summary

500

505

510

515

520

525

The data products described here provide annual updates to the global emissions and mole fraction trends, derived from measurements from the AGAGE network, routinely published in other scientific articles and assessments. The methodology and data inputs for deriving these data sets have been described in detail in one publication for the first time. The methodology will be updated along with emerging science, including, but not limited to, updated estimates of lifetimes and updated a priori emissions estimates. The aim will be for the methodology to remain consistent with future iterations of the World Meteorological Organisation's quadrennial Scientific Assessment of Ozone Depletion and other relevant assessments.

Global emissions, mole fractions, and their growth rates derived using AGAGE measurements and a 12-box model remain in widespread use. More complex transport models combined with AGAGE measurements are likely to complement the data

sets provided here (e.g., Western et al., 2024a; Liu et al., 2024), although we anticipate that the use of the 12-box model will remain in use for many years to come, due to its efficient and ease of use in this application.

9 Code and data availability

535

545

550

555

All AGAGE derived data sets presented in the paper are available at https://doi.org/10.5281/zenodo.15372480 (Western et al., 2025). Users must agree to the AGAGE Data Policy, the details of which can be found when downloading the data sets. The monthly mean measurements for each site used as input to the 12-box model are available at Prinn et al. (2025). The 12-box model and its inversion code are available from Rigby and Western (2022a) and Rigby and Western (2022b), respectively, or from https://github.com/mrghg/py12box and https://github.com/mrghg/py12box invert (both accessed on 8 May 2025).

Author contributions. LMW led the writing of the manuscript, with substantial contributions from JM, ALG and MR, and contributions from PJF, PBK, SR, KS, MKV and RGP. PJF, ALG, CMH, OH, JK, PBK, CRL, RLL, ZL, BM, JM, SO'D, JRP, SR, PKS, RS, KS, ARV,
 540 MKV, HJW, DY, and RFW provided measurement data, its calibration and quality control. HJW produced the monthly mean baselines. RGP and RFW oversee the AGAGE project. MR, HJW, JRP, LMW, ALG, BA, PKS, JM, PBK and MKV have curated the data.

Competing interests. The authors declare that they have no conflict of interest.

Acknowledgements. We would like to thank the continued support and efforts of the station operators, without whom this work would not be possible. We thank the NASA Upper Atmosphere Research Program for its continuing support of AGAGE through grants NNX07AE89G, NNX16AC98G and 80NSSC21K1369 to MIT and NNX07AF09G, NNX07AE87G, NNX16AC96G, NNX16AC97G, 80NSSC21K1210 and 80NSSC21K1201 to SIO to SIO and earlier grants. The Department for Energy Security and Net Zero (DESNZ) in the United Kingdom supported the University of Bristol for operations at Mace Head, Ireland (contracts 1028/06/2015, 1537/06/2018 and 5488/11/2021) and through the NASA award to MIT with the subaward to University of Bristol for Mace Head and Barbados (80NSSC21K1369). The National Oceanic and Atmospheric Administration (NOAA) in the United States supported the University of Bristol for operations at Ragged Point, Barbados (contract 1305M319CNRMJ0028) and operations at Cape Matatula, American Samoa. In Australia, the Kennaook/Cape Grim operations were supported by the Commonwealth Scientific and Industrial Research Organization (CSIRO), the Bureau of Meteorology (Australia), the Department of Climate Change, Energy, the Environment and Water (Australia), Refrigerant Reclaim Australia, the Australian Refrigeration Council and through the NASA award to MIT with subaward to CSIRO for Cape Grim (80NSSC21K1369). Measurements at Jungfraujoch are supported by the Swiss National Programs HALCLIM and CLIMGAS-CH (Swiss Federal Office for the Environment, FOEN), by the International Foundation High Altitude Research Stations Jungfraujoch and Gornergrat (HFSJG), and by the European infrastructure projects ICOS and ACTRIS. Measurements at Zeppelin are supported by the Norwegian Environment Agency.

References

- Adam, B., Western, L. M., Mühle, J., Choi, H., Krummel, P. B., O'Doherty, S., Young, D., Stanley, K. M., Fraser, P. J., Harth, C. M., Salameh, P. K., Weiss, R. F., Prinn, R. G., Kim, J., Park, H., Park, S., and Rigby, M.: Emissions of HFC-23 do not reflect commitments made under the Kigali Amendment, Communications Earth & Environment, 5, 1–8, https://doi.org/10.1038/s43247-024-01946-y, publisher: Nature Publishing Group, 2024.
 - An, M., Western, L. M., Say, D., Chen, L., Claxton, T., Ganesan, A. L., Hossaini, R., Krummel, P. B., Manning, A. J., Mühle, J., O'Doherty, S., Prinn, R. G., Weiss, R. F., Young, D., Hu, J., Yao, B., and Rigby, M.: Rapid increase in dichloromethane emissions from China inferred through atmospheric observations, Nature Communications, 12, 7279, https://doi.org/10.1038/s41467-021-27592-y, 2021.
- An, M., Western, L. M., Hu, J., Yao, B., Mühle, J., Ganesan, A. L., Prinn, R. G., Krummel, P. B., Hossaini, R., Fang, X., O'Doherty, S., Weiss, R. F., Young, D., and Rigby, M.: Anthropogenic Chloroform Emissions from China Drive Changes in Global Emissions, Environmental Science & Technology, 57, 13 925–13 936, https://doi.org/10.1021/acs.est.3c01898, 2023.
 - Arnold, T., Mühle, J., Salameh, P. K., Harth, C. M., Ivy, D. J., and Weiss, R. F.: Automated Measurement of Nitrogen Trifluoride in Ambient Air, Analytical Chemistry, 84, 4798–4804, https://doi.org/10.1021/ac300373e, 2012.
- Arnold, T., Harth, C. M., Mühle, J., Manning, A. J., Salameh, P. K., Kim, J., Ivy, D. J., Steele, L. P., Petrenko, V. V., Severinghaus, J. P., Baggenstos, D., and Weiss, R. F.: Nitrogen trifluoride global emissions estimated from updated atmospheric measurements, Proceedings of the National Academy of Sciences, 110, 2029–2034, https://doi.org/10.1073/pnas.1212346110, 2013.
 - Arnold, T., Ivy, D. J., Harth, C. M., Vollmer, M. K., Mühle, J., Salameh, P. K., Paul Steele, L., Krummel, P. B., Wang, R. H. J., Young, D., Lunder, C. R., Hermansen, O., Rhee, T. S., Kim, J., Reimann, S., O'Doherty, S., Fraser, P. J., Simmonds, P. G., Prinn, R. G., and Weiss, R. F.: HFC-43-10mee atmospheric abundances and global emission estimates, Geophysical Research Letters, 41, 2228–2235,
- Weiss, R. F.: HFC-43-10mee atmospheric abundances and global emission estimates, Geophysical Research Letters, 41, 2228-https://doi.org/10.1002/2013GL059143, _eprint: https://onlinelibrary.wiley.com/doi/pdf/10.1002/2013GL059143, 2014.
 - Ashford, P., Clodic, D., McCulloch, A., and Kuijpers, L.: Determination of comparative HCFC and HFC emission profiles for the foam and refrigeration sectors until 2015: Part 3: Total Emissions and Global Atmospheric Concentrations, 2004.
- Bloom, A. A., Bowman, K. W., Lee, M., Turner, A. J., Schroeder, R., Worden, J. R., Weidner, R., McDonald, K. C., and Jacob, D. J.: A global wetland methane emissions and uncertainty dataset for atmospheric chemical transport models (WetCHARTs version 1.0), Geoscientific Model Development, 10, 2141–2156, https://doi.org/10.5194/gmd-10-2141-2017, 2017.
 - Burkholder, J., Sander, S., Abbatt, J., Barker, J., Cappa, C., Crounse, J., Dibble, T., Huie, R., Kolb, C., Kurylo, M., Orkin, V., Percival, C., Wilmouth, D., and Wine, P.: Chemical kinetics and photochemical data for use in atmospheric studies; evaluation number 19, https://hdl.handle.net/2014/49199, edition: V1 Section: 2020-05-01 00:00:00.0, 2020.
- Burkholder, J. B. and Hodnebrog, Ø.: Summary of Abundances, Lifetimes, ODPs, REs, GWPs, and GTPs, in: Scientific Assessment of Ozone Depletion: 2022, World Meteorological Organization, Geneva, Switzerland, 2023.
 - Butcher, J. C.: A history of Runge-Kutta methods, Applied Numerical Mathematics, 20, 247–260, https://doi.org/10.1016/0168-9274(95)00108-5, 1996.
- Carpenter, L. C. and Reimann, S.: Update on Ozone-Depleting Substances (ODSs) and Other Gases of Interest to the Montreal Protocol, in:

 Scientific Assessment of Ozone Depletion: 2014, Project–Report No. 55, World Meteorological Organization, Geneva, Switzerland, 2014.
 - Crippa, M., Guizzardi, D., Pagani, F., Banja, M., Muntean, M., Schaaf, E., Becker, W., Monforti-Ferrario, F., Quadrelli, R., Risquez Martin, A., Taghavi-Moharamli, P., Köykkä, J., Grassi, G., Rossi, S., Brandao De Melo, J., Oom, D., Branco, A., San-Miguel, J., and Vignati, E.: GHG emissions of all world countries, Publications Office of the European Union, https://doi.org/10.2760/953322, 2023.

- Cunnold, D. M., Prinn, R. G., Rasmussen, R. A., Simmonds, P. G., Alyea, F. N., Cardelino, C. A., Crawford, A. J., Fraser,
 P. J., and Rosen, R. D.: The Atmospheric Lifetime Experiment: 3. Lifetime methodology and application to three years
 of CFCl₃ data, Journal of Geophysical Research: Oceans, 88, 8379–8400, https://doi.org/10.1029/JC088iC13p08379, _eprint:
 https://agupubs.onlinelibrary.wiley.com/doi/pdf/10.1029/JC088iC13p08379, 1983.
- Cunnold, D. M., Fraser, P. J., Weiss, R. F., Prinn, R. G., Simmonds, P. G., Miller, B. R., Alyea, F. N., and Crawford, A. J.:
 Global trends and annual releases of CCl₃F and CCl₂F₂ estimated from ALE/GAGE and other measurements from July
 1978 to June 1991, Journal of Geophysical Research: Atmospheres, 99, 1107–1126, https://doi.org/10.1029/93JD02715, _eprint:
 https://onlinelibrary.wiley.com/doi/pdf/10.1029/93JD02715, 1994.
 - Daniel, J. S. and Reimann, S.: Scenarios and Information for Policymakers, in: Scientific Assessment of Ozone Depletion: 2022, GAW Report No. 278, World Meteorological Organization, Geneva, Switzerland, 2023.
- Dlugokencky, E. J., Myers, R. C., Lang, P. M., Masarie, K. A., Crotwell, A. M., Thoning, K. W., Hall, B. D., Elkins, J. W., and Steele,

 L. P.: Conversion of NOAA atmospheric dry air CH₄ mole fractions to a gravimetrically prepared standard scale, Journal of Geophysical

 Research: Atmospheres, 110, 2005JD006 035, https://doi.org/10.1029/2005JD006035, 2005.
 - Ehhalt, D. H. and Fraser, P. J.: Trends in Source Gases, in: Report of the International Ozone Trends Panel 1988, vol. 1, United Nations Environment Program, Nairobi, Kenya, https://csl.noaa.gov/assessments/ozone/1988/report.html, 1988.
- Emmons, L. K., Walters, S., Hess, P. G., Guenther, A., Kinnison, D., Laepple, T., Orlando, J., Tie, X., Tyndall, G., Wiedinmyer, C., Baughcum,
 S. L., and Kloster, S.: Description and evaluation of the Model for Ozone and Related chemical Tracers, version 4 (MOZART-4), Geosci.
 Model Dev., p. 25, 2010.
 - Fang, X., Park, S., Saito, T., Tunnicliffe, R., Ganesan, A. L., Rigby, M., Li, S., Yokouchi, Y., Fraser, P. J., Harth, C. M., Krummel, P. B., Mühle, J., O'Doherty, S., Salameh, P. K., Simmonds, P. G., Weiss, R. F., Young, D., Lunt, M. F., Manning, A. J., Gressent, A., and Prinn, R. G.: Rapid increase in ozone-depleting chloroform emissions from China, Nature Geoscience, 12, 89–93, https://doi.org/10.1038/s41561-018-0278-2, 2019.

- Feng, L., Palmer, P. I., Parker, R. J., Lunt, M. F., and Bösch, H.: Methane emissions are predominantly responsible for record-breaking atmospheric methane growth rates in 2020 and 2021, Atmospheric Chemistry and Physics, 23, 4863–4880, https://doi.org/10.5194/acp-23-4863-2023, publisher: Copernicus GmbH, 2023.
- Fortems-Cheiney, A., Saunois, M., Pison, I., Chevallier, F., Bousquet, P., Cressot, C., Montzka, S. A., Fraser, P. J., Vollmer, M. K., Simmonds,
 P. G., Young, D., O'Doherty, S., Weiss, R. F., Artuso, F., Barletta, B., Blake, D. R., Li, S., Lunder, C., Miller, B. R., Park, S., Prinn, R.,
 Saito, T., Steele, L. P., and Yokouchi, Y.: Increase in HFC-134a emissions in response to the success of the Montreal Protocol, Journal of Geophysical Research: Atmospheres, 120, https://doi.org/10.1002/2015JD023741, 2015.
 - Fraser, P. J., Langenfelds, R. L., Derek, N., and Porter, L. W.: Studies in air archiving techniques, in: Baseline Atmospheric Program (Australia) 1989, edited by Wilson, S. R. and Gras, J. L., pp. 16–29, Department of the Arts, Sport, the Environment, Tourism and Territories, Bureau of Meteorology and CSIRO Division of Atmospheric Research, Canberra, A.C.T., 1991.
 - Fraser, P. J., Dunse, B. L., Manning, A. J., Walsh, S., Wang, R. H. J., Krummel, P. B., Steele, L. P., Porter, L. W., Allison, C., O'Doherty, S., Simmonds, P. G., Mühle, J., Weiss, R. F., and Prinn, R. G.: Australian carbon tetrachloride emissions in a global context, Environmental Chemistry, 11, 77, https://doi.org/10.1071/EN13171, 2014.
- Fraser, P. J., Pearman, G. I., and Derek, N.: CSIRO Non-carbon Dioxide Greenhouse Gas Research. Part 1: 1975–90, Historical Records of Australian Science, 29, 1, https://doi.org/10.1071/HR17016, 2018.

- Fung, I., John, J., Lerner, J., Matthews, E., Prather, M., Steele, L. P., and Fraser, P. J.: Three-dimensional model synthesis of the global methane cycle, Journal of Geophysical Research: Atmospheres, 96, 13 033–13 065, https://doi.org/10.1029/91JD01247, _eprint: https://onlinelibrary.wiley.com/doi/pdf/10.1029/91JD01247, 1991.
- Ganesan, A. L., Rigby, M., Zammit-Mangion, A., Manning, A. J., Prinn, R. G., Fraser, P. J., Harth, C. M., Kim, K.-R., Krummel, P. B., Li, S.,
 Mühle, J., O'Doherty, S. J., Park, S., Salameh, P. K., Steele, L. P., and Weiss, R. F.: Characterization of uncertainties in atmospheric trace gas inversions using hierarchical Bayesian methods, Atmospheric Chemistry and Physics, 14, 3855–3864, https://doi.org/10.5194/acp-14-3855-2014, 2014.
 - Golombek, A. and Prinn, R. G.: A global three-dimensional model of the circulation and chemistry of CFCl₃, CF₂Cl₂, CH₃CCl₃, CCl₄, and N₂O, Journal of Geophysical Research: Atmospheres, 91, 3985–4001, https://doi.org/10.1029/JD091iD03p03985, _eprint: https://onlinelibrary.wilev.com/doi/pdf/10.1029/JD091iD03p03985, 1986.

660

- Gulev, S. K. and Thorne, P. W.: Climate Change 2021 The Physical Science Basis: Working Group I Contribution to the Sixth Assessment Report of the Intergovernmental Panel on Climate Change, Cambridge University Press, 1 edn., https://doi.org/10.1017/9781009157896, 2023.
- Gütschow, J., Jeffery, M. L., Gieseke, R., Gebel, R., Stevens, D., Krapp, M., and Rocha, M.: The PRIMAP-hist national historical emissions time series, Earth System Science Data, 8, 571–603, https://doi.org/10.5194/essd-8-571-2016, 2016.
 - Gütschow, J., Busch, D., and Pflüger, M.: The PRIMAP-hist national historical emissions time series (1750-2023) v2.6, https://doi.org/10.5281/ZENODO.13752654, 2024.
 - Hodnebrog, Ø., Myhre, G., Kramer, R. J., Shine, K. P., Andrews, T., Faluvegi, G., Kasoar, M., Kirkevåg, A., Lamarque, J.-F., Mülmenstädt, J., Olivié, D., Samset, B. H., Shindell, D., Smith, C. J., Takemura, T., and Voulgarakis, A.: The effect of rapid adjustments to halocarbons and Na O on radiative forcing, ppi Climate and Atmospheric Science, 3, 1–7, https://doi.org/10.1038/s41612-020-00150-x, publisher: Nature
- N₂O on radiative forcing, npj Climate and Atmospheric Science, 3, 1–7, https://doi.org/10.1038/s41612-020-00150-x, publisher: Nature Publishing Group, 2020.
 - HTOC: Report of the UNEP Halons Technical Options Committee December 2014, vol. 1, UNEP, Nairobi, Kenya, 2014.
 - IPCC, Houghton, J. T., Jenkins, G. J., Ephraums, J. J., and Intergovernmental Panel on Climate Change, eds.: Climate change: the IPCC scientific assessment, Cambridge University Press, Cambridge; New York, 1990.
- Ivy, D. J., Arnold, T., Harth, C. M., Steele, L. P., Mühle, J., Rigby, M., Salameh, P. K., Leist, M., Krummel, P. B., Fraser, P. J., Weiss, R. F., and Prinn, R. G.: Atmospheric histories and growth trends of C₄F₁0, C₅F₁₂, C₆F₁₄, C₇F₁₆ and C₈F₁₈, Atmospheric Chemistry and Physics, 12, 4313–4325, https://doi.org/10.5194/acp-12-4313-2012, 2012.
 - Jackson, R. B., Saunois, M., Bousquet, P., Canadell, J. G., Poulter, B., Stavert, A. R., Bergamaschi, P., Niwa, Y., Segers, A., and Tsuruta, A.: Increasing anthropogenic methane emissions arise equally from agricultural and fossil fuel sources, Environmental Research Letters, 15, 071 002, https://doi.org/10.1088/1748-9326/ab9ed2, publisher: IOP Publishing, 2020.
 - Kalnay, E., Kanamitsu, M., Kistler, R., Collins, W., Deaven, D., Gandin, L., Iredell, M., Saha, S., White, G., Woollen, J., Zhu, Y., Chelliah, M., Ebisuzaki, W., Higgins, W., Janowiak, J., Mo, K. C., Ropelewski, C., Wang, J., Leetmaa, A., Reynolds, R., Jenne, R., and Joseph, D.: The NCEP/NCAR 40-Year Reanalysis Project, Bulletin of the American Meteorological Society, 77, 437–472, https://doi.org/10.1175/1520-0477(1996)077<0437:TNYRP>2.0.CO;2, publisher: American Meteorological Society Section: Bulletin of the American Meteorological Society, 1996.
 - Keene, W. C., Khalil, M. A. K., Erickson III, D. J., McCulloch, A., Graedel, T. E., Lobert, J. M., Aucott, M. L., Gong, S. L., Harper, D. B., Kleiman, G., Midgley, P., Moore, R. M., Seuzaret, C., Sturges, W. T., Benkovitz, C. M., Koropalov, V., Barrie, L. A., and Li, Y. F.: Composite global emissions of reactive chlorine from anthropogenic and natural sources: Reactive Chlorine

- Emissions Inventory, Journal of Geophysical Research: Atmospheres, 104, 8429–8440, https://doi.org/10.1029/1998JD100084, _eprint: https://onlinelibrary.wiley.com/doi/pdf/10.1029/1998JD100084, 1999.
 - Ko, M. K. W., Newman, P. A., Reimann, S., and Strahan, S. E.: SPARC Report on Lifetimes of Stratospheric Ozone-Depleting Substances, Their Replacements, and Related Species, Tech. rep., SPARC Office, http://www.sparc-climate.org/publications/sparc-reports/, backup Publisher: SPARC Publication Title: SPARC Report Volume: No. 6, 2013.
- Langenfelds, R. L., Fraser, P. J., Francey, R. J., Steele, L. P., Porter, L. W., and Allison, C. E.: Baseline Atmospheric Program Australia 1994-95, Bureau of Meteorology and CSIRO Division of Atmospheric Research, https://doi.org/10.4225/08/5865509FA7A35, publisher: [Melbourne], Bureau of Meteorology and CSIRO Division of Atmospheric Research, 1996.
 - Laube, J. C. and Tegtmeier: Update on Ozone-Depleting Substances (ODSs) and Other Gases of Interest to the Montreal Protocol, in: Scientific Assessment of Ozone Depletion: 2022, GAW Report No. 278, World Meteorological Organization, Geneva, Switzerland, 2023.
 - Liang, Q. and Rigby, M.: Hydrofluorocarbons (HFCs), in: Scientific Assessment of Ozone Depletion: 2022, GAW Report No. 278, World Meteorological Organization, Geneva, Switzerland, 2023.

- Liang, Q., Newman, P. A., and Reimann, S.: SPARC Report on the Mystery of Carbon Tetrachloride, Tech. rep., ETH Zurich, https://doi.org/10.3929/ETHZ-A-010690647, medium: application/pdf,1 Online-Ressource, 2016.
- Lickley, M., Fletcher, S., Rigby, M., and Solomon, S.: Joint inference of CFC lifetimes and banks suggests previously unidentified emissions, Nature Communications, 12, 2920, https://doi.org/10.1038/s41467-021-23229-2, 2021.
- Liu, Y., Sheng, J., Rigby, M., Ganesan, A., Kim, J., Western, L. M., Mühle, J., Park, S., Park, H., Weiss, R. F., Salameh, P. K., O'Doherty, S., Young, D., Krummel, P. B., Vollmer, M. K., Reimann, S., Lunder, C. R., and Prinn, R. G.: Increases in Global and East Asian Nitrogen Trifluoride (NF 3) Emissions Inferred from Atmospheric Observations, Environmental Science & Technology, p. acs.est.4c04507, https://doi.org/10.1021/acs.est.4c04507, 2024.
- Lunt, M. F., Rigby, M., Ganesan, A. L., Manning, A. J., Prinn, R. G., O'Doherty, S., Mühle, J., Harth, C. M., Salameh, P. K., Arnold,
 T., Weiss, R. F., Saito, T., Yokouchi, Y., Krummel, P. B., Steele, L. P., Fraser, P. J., Li, S., Park, S., Reimann, S., Vollmer, M. K.,
 Lunder, C., Hermansen, O., Schmidbauer, N., Maione, M., Arduini, J., Young, D., and Simmonds, P. G.: Reconciling reported and unreported HFC emissions with atmospheric observations, Proceedings of the National Academy of Sciences, 112, 5927–5931, https://doi.org/10.1073/pnas.1420247112, 2015.
- Manning, A. J., Redington, A. L., Say, D., O'Doherty, S., Young, D., Simmonds, P. G., Vollmer, M. K., Mühle, J., Arduini, J., Spain,
 G., Wisher, A., Maione, M., Schuck, T. J., Stanley, K., Reimann, S., Engel, A., Krummel, P. B., Fraser, P. J., Harth, C. M., Salameh,
 P. K., Weiss, R. F., Gluckman, R., Brown, P. N., Watterson, J. D., and Arnold, T.: Evidence of a recent decline in UK emissions of hydrofluorocarbons determined by the InTEM inverse model and atmospheric measurements, Atmospheric Chemistry and Physics, 21, 12739–12755, https://doi.org/10.5194/acp-21-12739-2021, 2021.
- McCulloch, A.: Chloroform in the environment: occurrence, sources, sinks and effects, Chemosphere, 50, 1291–1308, https://doi.org/10.1016/S0045-6535(02)00697-5, 2003.
 - McCulloch, A., Aucott, M. L., Graedel, T. E., Kleiman, G., Midgley, P. M., and Li, Y.-F.: Industrial emissions of trichloroethene, tetra-chloroethene, and dichloromethane: Reactive Chlorine Emissions Inventory, Journal of Geophysical Research: Atmospheres, 104, 8417–8427, https://doi.org/10.1029/1999JD900011, _eprint: https://onlinelibrary.wiley.com/doi/pdf/10.1029/1999JD900011, 1999.
- McCulloch, A., Ashford, P., and Midgley, P. M.: Historic emissions of fluorotrichloromethane (CFC-11) based on a market survey, Atmospheric Environment, 35, 4387–4397, https://doi.org/10.1016/S1352-2310(01)00249-7, 2001.

- McCulloch, A., Midgley, P. M., and Ashford, P.: Releases of refrigerant gases (CFC-12, HCFC-22 and HFC-134a) to the atmosphere, Atmospheric Environment, 37, 889–902, https://doi.org/10.1016/S1352-2310(02)00975-5, 2003.
- McGillen, M. R., Fried, Z. T. P., Khan, M. A. H., Kuwata, K. T., Martin, C. M., O'Doherty, S., Pecere, F., Shallcross, D. E., Stanley, K. M., and Zhang, K.: Ozonolysis can produce long-lived greenhouse gases from commercial refrigerants, Proceedings of the National Academy of Sciences, 120, e2312714120, https://doi.org/10.1073/pnas.2312714120, publisher: Proceedings of the National Academy of Sciences,
- Meinshausen, M., Nicholls, Z. R. J., Lewis, J., Gidden, M. J., Vogel, E., Freund, M., Beyerle, U., Gessner, C., Nauels, A., Bauer, N., Canadell, J. G., Daniel, J. S., John, A., Krummel, P. B., Luderer, G., Meinshausen, N., Montzka, S. A., Rayner, P. J., Reimann, S., Smith, S. J., van den Berg, M., Velders, G. J. M., Vollmer, M. K., and Wang, R. H. J.: The shared socio-economic pathway (SSP) greenhouse gas concentrations and their extensions to 2500, Geoscientific Model Development, 13, 3571–3605, https://doi.org/10.5194/gmd-13-3571-2020, publisher: Copernicus GmbH, 2020.
- Miller, B. R., Huang, J., Weiss, R. F., Prinn, R. G., and Fraser, P. J.: Atmospheric trend and lifetime of chlorodifluoromethane (HCFC-22) and the global tropospheric OH concentration, Journal of Geophysical Research: Atmospheres, 103, 13 237–13 248, https://doi.org/10.1029/98JD00771, 1998.
- Miller, B. R., Weiss, R. F., Salameh, P. K., Tanhua, T., Greally, B. R., Muhle, J., and Simmonds, P. G.: Medusa: A Sample Preconcentration and GC / MS Detector System for in Situ Measurements of Atmospheric Trace Halocarbons, Hydrocarbons, and Sulfur Compounds, Analytical Chemistry, 80, 1536–1545, https://doi.org/10.1029/2004GL022228.(8), 2008.
 - Miller, B. R., Rigby, M., Kuijpers, L. J. M., Krummel, P. B., Steele, L. P., Leist, M., Fraser, P. J., McCulloch, A., Harth, C., Salameh, P., Mühle, J., Weiss, R. F., Prinn, R. G., Wang, R. H. J., O'Doherty, S., Greally, B. R., and Simmonds, P. G.: HFC-23 (CHF₃) emission trend response to HCFC-22 (CHClF₂) production and recent HFC-23 emission abatement measures, Atmospheric Chemistry and Physics, 10,
 - 7875–7890, https://doi.org/10.5194/acp-10-7875-2010, publisher: Copernicus GmbH, 2010.

715

725

2023.

- Montzka, S., Vimont, I., Hall, B., and Clingan, S.: Making atmospheric measurements of difficult-to-separate isomers of CFCs routine: a case study of CFC-113 and CFC-113a that refines our understanding of recent atmospheric changes for both of these chemicals., https://doi.org/10.5194/egusphere-egu24-19613, 2025.
- Montzka, S. A. and Reimann, S.: Ozone-Depleting Substances (ODSs) and Related Chemicals, in: Scientific Assessment of Ozone Depletion: 2010, World Meteorological Organization, 2010.
 - Montzka, S. A., Butler, J. H., Myers, R. C., Thompson, T. M., Swanson, T. H., Clarke, A. D., Lock, L. T., and Elkins, J. W.: Decline in the Tropospheric Abundance of Halogen from Halocarbons: Implications for Stratospheric Ozone Depletion, Science, 272, 1318–1322, https://doi.org/10.1126/science.272.5266.1318, 1996.
- Montzka, S. A., Dutton, G. S., Yu, P., Ray, E., Portmann, R. W., Daniel, J. S., Kuijpers, L., Hall, B. D., Mondeel, D., Siso, C., Nance, J. D., Rigby, M., Manning, A. J., Hu, L., Moore, F., Miller, B. R., and Elkins, J. W.: An unexpected and persistent increase in global emissions of ozone-depleting CFC-11, Nature, 557, 413–417, https://doi.org/10.1038/s41586-018-0106-2, 2018.
 - Montzka, S. A., Dutton, G. S., Portmann, R. W., Chipperfield, M. P., Davis, S., Feng, W., Manning, A. J., Ray, E., Rigby, M., Hall, B. D., Siso, C., Nance, J. D., Krummel, P. B., Mühle, J., Young, D., O'Doherty, S., Salameh, P. K., Harth, C. M., Prinn, R. G., Weiss, R. F.,
- Elkins, J. W., Walter-Terrinoni, H., and Theodoridi, C.: A decline in global CFC-11 emissions during 2018-2019, Nature, 590, 428–432, https://doi.org/10.1038/s41586-021-03260-5, number: 7846 Publisher: Nature Publishing Group, 2021.

- Myhre, G., Shindell, D., Bréon, F.-M., Collins, W., Fuglestvedt, J., Huang, J., Koch, D., Lamarque, J.-F., Lee, D., Mendoza, B., Nakajima, T., Robock, A., Stephens, G., Takemura, T., and Zhang, H.: A and natural radiative forcing, Climate Change 2013-The Physical Science Basis, pp. 659–740, 2014.
- Mühle, J., Huang, J., Weiss, R. F., Prinn, R. G., Miller, B. R., Salameh, P. K., Harth, C. M., Fraser, P. J., Porter, L. W., Greally, B. R., O'Doherty, S., and Simmonds, P. G.: Sulfuryl fluoride in the global atmosphere, Journal of Geophysical Research: Atmospheres, 114, https://doi.org/10.1029/2008JD011162, _eprint: https://onlinelibrary.wiley.com/doi/pdf/10.1029/2008JD011162, 2009.
 - Mühle, J., Ganesan, A. L., Miller, B. R., Salameh, P. K., Harth, C. M., Greally, B. R., Rigby, M., Porter, L. W., Steele, L. P., Trudinger, C. M., Krummel, P. B., O'Doherty, S., Fraser, P. J., Simmonds, P. G., Prinn, R. G., and Weiss, R. F.: Perfluorocarbons in the global atmosphere: tetrafluoromethane, hexafluoroethane, and octafluoropropane. Atmospheric Chemistry and Physics, 10, 5145–5164.
- global atmosphere: tetrafluoromethane, hexafluoroethane, and octafluoropropane, Atmospheric Chemistry and Physics, 10, 5145–5164, https://doi.org/10.5194/acp-10-5145-2010, 2010.
 - Mühle, J., Trudinger, C. M., Western, L. M., Rigby, M., Vollmer, M. K., Park, S., Manning, A. J., Say, D., Ganesan, A., Steele, L. P., Ivy, D. J., Arnold, T., Li, S., Stohl, A., Harth, C. M., Salameh, P. K., McCulloch, A., O'Doherty, S., Park, M.-K., Jo, C. O., Young, D., Stanley, K. M., Krummel, P. B., Mitrevski, B., Hermansen, O., Lunder, C., Evangeliou, N., Yao, B., Kim, J., Hmiel, B.,
- Buizert, C., Petrenko, V. V., Arduini, J., Maione, M., Etheridge, D. M., Michalopoulou, E., Czerniak, M., Severinghaus, J. P., Reimann, S., Simmonds, P. G., Fraser, P. J., Prinn, R. G., and Weiss, R. F.: Perfluorocyclobutane (PFC-318, c-C₄F₈) in the global atmosphere, Atmospheric Chemistry and Physics, 19, 10 335–10 359, https://doi.org/10.5194/acp-19-10335-2019, 2019.
 - Mühle, J., Kuijpers, L. J. M., Stanley, K. M., Rigby, M., Western, L. M., Kim, J., Park, S., Harth, C. M., Krummel, P. B., Fraser, P. J., O'Doherty, S., Salameh, P. K., Schmidt, R., Young, D., Prinn, R. G., Wang, R. H. J., and Weiss, R. F.: Global emissions of perfluorocy-
- clobutane (PFC-318, c-C₄F₈) resulting from the use of hydrochlorofluorocarbon-22 (HCFC-22) feedstock to produce polytetrafluoroethylene (PTFE) and related fluorochemicals, Atmospheric Chemistry and Physics, 22, 3371–3378, https://doi.org/10.5194/acp-22-3371-2022, 2022.

- Mühle, J., Adam, B., Miller, B. R., Ivy, D., Arnold, T., Vollmer, M., Weiss, R., Western, L., Rigby, M., Krummel, P., Fraser, P., Steele, P., and Langenfelds, R.: AGAGE measurements of atmospheric trace gases from archived air samples., https://doi.org/10.5281/ZENODO.16926034, 2025.
- Naus, S., Montzka, S. A., Pandey, S., Basu, S., Dlugokencky, E. J., and Krol, M.: Constraints and biases in a tropospheric two-box model of OH, Atmospheric Chemistry and Physics, 19, 407–424, https://doi.org/10.5194/acp-19-407-2019, 2019.
- Newell, R. E., Vincent, D. G., and Kidson, J. W.: Interhemispheric mass exchange from meteorological and trace substance observations, Tellus, 21, 641–647, https://doi.org/10.1111/j.2153-3490.1969.tb00471.x, 1969.
- Nisbet, E. G., Dlugokencky, E. J., Manning, M. R., Lowry, D., Fisher, R. E., France, J. L., Michel, S. E., Miller, J. B., White, J. W. C., Vaughn, B., Bousquet, P., Pyle, J. A., Warwick, N. J., Cain, M., Brownlow, R., Zazzeri, G., Lanoisellé, M., Manning, A. C., Gloor, E., Worthy, D. E. J., Brunke, E.-G., Labuschagne, C., Wolff, E. W., and Ganesan, A. L.: Rising atmospheric methane: 2007-2014 growth and isotopic shift, Global Biogeochemical Cycles, 30, 1356–1370, https://doi.org/10.1002/2016GB005406, 2016.
- O'Doherty, S., Simmonds, P. G., Cunnold, D. M., Wang, H. J., Sturrock, G. A., Fraser, P. J., Ryall, D., Derwent, R. G., Weiss, R. F., Salameh, P., Miller, B. R., and Prinn, R. G.: In situ chloroform measurements at Advanced Global Atmospheric Gases Experiment atmospheric research stations from 1994 to 1998, Journal of Geophysical Research: Atmospheres, 106, 20429–20444, https://doi.org/10.1029/2000JD900792, eprint: https://onlinelibrary.wiley.com/doi/pdf/10.1029/2000JD900792, 2001.
 - O'Doherty, S., Cunnold, D. M., Manning, A., Miller, B. R., Wang, R. H. J., Krummel, P. B., Fraser, P. J., Simmonds, P. G., McCulloch, A., Weiss, R. F., Salameh, P., Porter, L. W., Prinn, R. G., Huang, J., Sturrock, G., Ryall, D., Derwent, R. G., and Montzka, S. A.:

- Rapid growth of hydrofluorocarbon 134a and hydrochlorofluorocarbons 141b, 142b, and 22 from Advanced Global Atmospheric Gases Experiment (AGAGE) observations at Cape Grim, Tasmania, and Mace Head, Ireland, Journal of Geophysical Research: Atmospheres, 109, https://doi.org/10.1029/2003JD004277, _eprint: https://onlinelibrary.wiley.com/doi/pdf/10.1029/2003JD004277, 2004.
 - O'Doherty, S., Cunnold, D. M., Miller, B. R., Mühle, J., McCulloch, A., Simmonds, P. G., Manning, A. J., Reimann, S., Vollmer, M. K., Greally, B. R., Prinn, R. G., Fraser, P. J., Steele, L. P., Krummel, P. B., Dunse, B. L., Porter, L. W., Lunder, C. R., Schmidbauer, N.,
- Hermansen, O., Salameh, P. K., Harth, C. M., Wang, R. H. J., and Weiss, R. F.: Global and regional emissions of HFC-125 (CHF₂CF₃) from in situ and air archive atmospheric observations at AGAGE and SOGE observatories, Journal of Geophysical Research: Atmospheres, 114, https://doi.org/10.1029/2009JD012184, _eprint: https://onlinelibrary.wiley.com/doi/pdf/10.1029/2009JD012184, 2009.
 - O'Doherty, S., Rigby, M., Mühle, J., Ivy, D. J., Miller, B. R., Young, D., Simmonds, P. G., Reimann, S., Vollmer, M. K., Krummel, P. B., Fraser, P. J., Steele, L. P., Dunse, B., Salameh, P. K., Harth, C. M., Arnold, T., Weiss, R. F., Kim, J., Park, S., Li, S., Lunder, C., Hermansen, O., Schmidbauer, N., Zhou, L. X., Yao, B., Wang, R. H. J., Manning, A. J., and Prinn, R. G.: Global emissions of HFC-143a (CH₃CF₃) and HFC-32 (CH₂F₂) from in situ and air archive atmospheric observations, Atmospheric Chemistry and Physics, 14, 9249–

805

9258, https://doi.org/10.5194/acp-14-9249-2014, 2014.

- Park, S., Western, L. M., Saito, T., Redington, A. L., Henne, S., Fang, X., Prinn, R. G., Manning, A. J., Montzka, S. A., Fraser, P. J., Ganesan, A. L., Harth, C. M., Kim, J., Krummel, P. B., Liang, Q., Mühle, J., O'Doherty, S., Park, H., Park, M.-K., Reimann, S., Salameh,
- P. K., Weiss, R. F., and Rigby, M.: A decline in emissions of CFC-11 and related chemicals from eastern China, Nature, 590, 433–437, https://doi.org/10.1038/s41586-021-03277-w, number: 7846 Publisher: Nature Publishing Group, 2021.
 - Platt, S. M., Hov, , Berg, T., Breivik, K., Eckhardt, S., Eleftheriadis, K., Evangeliou, N., Fiebig, M., Fisher, R., Hansen, G., Hansson, H.-C., Heintzenberg, J., Hermansen, O., Heslin-Rees, D., Holmén, K., Hudson, S., Kallenborn, R., Krejci, R., Krognes, T., Larssen, S., Lowry, D., Lund Myhre, C., Lunder, C., Nisbet, E., Nizzetto, P. B., Park, K.-T., Pedersen, C. A., Aspmo Pfaffhuber, K., Röckmann, T., Schmidbauer,
- N., Solberg, S., Stohl, A., Ström, J., Svendby, T., Tunved, P., Tørnkvist, K., van der Veen, C., Vratolis, S., Yoon, Y. J., Yttri, K. E., Zieger, P., Aas, W., and Tørseth, K.: Atmospheric composition in the European Arctic and 30 years of the Zeppelin Observatory, Ny-Ålesund, Atmospheric Chemistry and Physics, 22, 3321–3369, https://doi.org/10.5194/acp-22-3321-2022, publisher: Copernicus GmbH, 2022.
 - Prinn, R., Weiss, R., Arduini, J., Arnold, T., DeWitt, H. L., Fraser, P., Ganesan, A., Gasore, J., Harth, C., Hermansen, O., Kim, J., Krummel, P., Loh, Z., Lunder, C., Maione, M., Manning, A., Miller, B., Mitrevski, B., JMühle, J., O'Doherty, S., Park, S., Reimann, S., Rigby, M., Saito, T., Salameh, P., Schmidt, R., Simmonds, P., Steele, P., Vollmer, M., Hsiang-Jui (Ray), W., Yao, B., Young, D., and Zhou, L.: The
 - Prinn, R., Weiss, R., Arduini, J., Choi, H., Engel, A., Fraser, P., Ganesan, A., Harth, C., Hermansen, O., Kim, J., Krummel, P., Lo, Z., Lunder, C., Maione, M., Manning, A., Mitrevski, B., Mühle, J., O'Doherty, S., Park, S., Pitt, J., Reimann, S., Rigby, M., Saito, T., Salameh, P., Schmidt, R., Simmonds, P., Stanley, K., Stavert, A., Steel, P., Vollmer, M., Wagenhäuser, T., Wang, H., Wenger, A., Western, L., Yao, B.,
- Young, D., Zhou, L., and Zhu, L.: The dataset of in-situ measurements of chemically and radiatively important atmospheric gases from the Advanced Global Atmospheric Gas Experiment (AGAGE) and affiliated stations, https://doi.org/10.60718/0FXA-QF43, 2025.

Advanced Global Atmospheric Gases Experiment (AGAGE) Data, https://doi.org/10.15485/1841748, 2022.

- Prinn, R. G., Rasmussen, R. A., Simmonds, P. G., Alyea, F. N., Cunnold, D. M., Lane, B. C., Cardelino, C. A., and Crawford, A. J.: The Atmospheric Lifetime Experiment: 5. Results for CH₃CCl₃ based on three years of data, Journal of Geophysical Research: Oceans, 88, 8415–8426, https://doi.org/10.1029/JC088iC13p08415, 1983a.
- 815 Prinn, R. G., Simmonds, P. G., Rasmussen, R. A., Rosen, R. D., Alyea, F. N., Cardelino, C. A., Crawford, A. J., Cunnold, D. M., Fraser, P. J., and Lovelock, J. E.: The Atmospheric Lifetime Experiment: 1. Introduction, instrumentation,

- and overview, Journal of Geophysical Research: Oceans, 88, 8353–8367, https://doi.org/10.1029/JC088iC13p08353, _eprint: https://onlinelibrary.wiley.com/doi/pdf/10.1029/JC088iC13p08353, 1983b.
- Prinn, R. G., Weiss, R. F., Miller, B. R., Huang, J., Alyea, F. N., Cunnold, D. M., Fraser, P. J., Hartley, D. E., and Simmonds, P. G.: Atmospheric Trends and Lifetime of CH₃CCl₃ and Global OH Concentrations, Science, 269, 187–192, https://doi.org/10.1126/science.269.5221.187, 1995.
 - Prinn, R. G., Weiss, R. F., Fraser, P. J., Simmonds, P. G., Cunnold, D. M., Alyea, F. N., O'Doherty, S., Salameh, P., Miller, B. R., Huang, J., Wang, R. H. J., Hartley, D. E., Harth, C., Steele, L. P., Sturrock, G., Midgley, P. M., and McCulloch, A.: A history of chemically and radiatively important gases in air deduced from ALE/GAGE/AGAGE, Journal of Geophysical Research: Atmospheres, 105, 17751–17792, https://doi.org/10.1029/2000JD900141, eprint: https://onlinelibrary.wiley.com/doi/pdf/10.1029/2000JD900141, 2000.

- Prinn, R. G., Huang, J., Weiss, R. F., Cunnold, D. M., Fraser, P. J., Simmonds, P. G., McCulloch, A., Harth, C., Reimann, S., Salameh, P., O'Doherty, S., Wang, R. H. J., Porter, L. W., Miller, B. R., and Krummel, P. B.: Evidence for variability of atmospheric hydroxyl radicals over the past quarter century, Geophysical Research Letters, 32, https://doi.org/10.1029/2004GL022228, 2005.
- Prinn, R. G., Weiss, R. F., Arduini, J., Arnold, T., DeWitt, H. L., Fraser, P. J., Ganesan, A. L., Gasore, J., Harth, C. M., Hermansen,
 O., Kim, J., Krummel, P. B., Li, S., Loh, Z. M., Lunder, C. R., Maione, M., Manning, A. J., Miller, B. R., Mitrevski, B., Mühle, J.,
 O'Doherty, S., Park, S., Reimann, S., Rigby, M., Saito, T., Salameh, P. K., Schmidt, R., Simmonds, P. G., Steele, L. P.,
 Vollmer, M. K., Wang, R. H., Yao, B., Yokouchi, Y., Young, D., and Zhou, L.: History of chemically and radiatively important atmospheric gases from the Advanced Global Atmospheric Gases Experiment (AGAGE), Earth System Science Data, 10, 985–1018, https://doi.org/10.5194/essd-10-985-2018, 2018.
- Ray, E. A., Portmann, R. W., Yu, P., Daniel, J., Montzka, S. A., Dutton, G. S., Hall, B. D., Moore, F. L., and Rosenlof, K. H.: The influence of the stratospheric Quasi-Biennial Oscillation on trace gas levels at the Earth's surface, Nature Geoscience, 13, 22–27, https://doi.org/10.1038/s41561-019-0507-3, 2020.
- Reimann, S., Schaub, D., Stemmler, K., Folini, D., Hill, M., Hofer, P., Buchmann, B., Simmonds, P. G., Greally, B. R., and O'Doherty, S.: Halogenated greenhouse gases at the Swiss High Alpine Site of Jungfraujoch (3580 m asl): Continuous measurements and their use for regional European source allocation, Journal of Geophysical Research: Atmospheres, 109, https://doi.org/10.1029/2003JD003923, eprint: https://onlinelibrary.wiley.com/doi/pdf/10.1029/2003JD003923, 2004.
 - Reimann, S., Vollmer, M. K., Folini, D., Steinbacher, M., Hill, M., Buchmann, B., Zander, R., and Mahieu, E.: Observations of long-lived anthropogenic halocarbons at the high-Alpine site of Jungfraujoch (Switzerland) for assessment of trends and European sources, Science of The Total Environment, 391, 224–231, https://doi.org/10.1016/j.scitotenv.2007.10.022, 2008.
- Resplandy, L., Hogikyan, A., Müller, J. D., Najjar, R. G., Bange, H. W., Bianchi, D., Weber, T., Cai, W.-J., Doney, S. C., Fennel, K., Gehlen, M., Hauck, J., Lacroix, F., Landschützer, P., Le Quéré, C., Roobaert, A., Schwinger, J., Berthet, S., Bopp, L., Chau, T. T. T., Dai, M., Gruber, N., Ilyina, T., Kock, A., Manizza, M., Lachkar, Z., Laruelle, G. G., Liao, E., Lima, I. D., Nissen, C., Rödenbeck, C., Séférian, R., Toyama, K., Tsujino, H., and Regnier, P.: A Synthesis of Global Coastal Ocean Greenhouse Gas Fluxes, Global Biogeochemical Cycles, 38, e2023GB007 803, https://doi.org/10.1029/2023GB007803, _eprint: https://onlinelibrary.wiley.com/doi/pdf/10.1029/2023GB007803,
 2024.
 - Rhew, R. C., Miller, B. R., and Weiss, R. F.: Natural methyl bromide and methyl chloride emissions from coastal salt marshes, Nature, 403, 292–295, https://doi.org/10.1038/35002043, publisher: Nature Publishing Group, 2000.
 - Rigby, M. and Western, L.: mrghg/py12box; v0.2.1, https://doi.org/10.5281/ZENODO.6857447, 2022a.
 - Rigby, M. and Western, L.: mrghg/py12box_invert: v0.0.2, https://doi.org/10.5281/ZENODO.6857794, 2022b.

- Rigby, M., Prinn, R. G., Fraser, P. J., Simmonds, P. G., Langenfelds, R. L., Huang, J., Cunnold, D. M., Steele, L. P., Krummel, P. B., Weiss, R. F., O'Doherty, S., Salameh, P. K., Wang, H. J., Harth, C. M., Mühle, J., and Porter, L. W.: Renewed growth of atmospheric methane, Geophysical Research Letters, 35, https://doi.org/10.1029/2008GL036037, 2008.
 - Rigby, M., Mühle, J., Miller, B. R., Prinn, R. G., Krummel, P. B., Steele, L. P., Fraser, P. J., Salameh, P. K., Harth, C. M., Weiss, R. F., Greally, B. R., O'Doherty, S., Simmonds, P. G., Vollmer, M. K., Reimann, S., Kim, J., Kim, K.-R., Wang, H. J., Olivier, J. G. J., Dlugokencky, D. J., Dirtter, G. S., Hall, B. D., and Ellving, L. W., History of the carbonic SE. from 1973 to 2008. At a carbonic School and Physics
- E. J., Dutton, G. S., Hall, B. D., and Elkins, J. W.: History of atmospheric SF₆ from 1973 to 2008, Atmospheric Chemistry and Physics, 10, 10 305–10 320, https://doi.org/10.5194/acp-10-10305-2010, publisher: Copernicus GmbH, 2010.
 - Rigby, M., Ganesan, A. L., and Prinn, R. G.: Deriving emissions time series from sparse atmospheric mole fractions, Journal of Geophysical Research: Atmospheres, 116, https://doi.org/10.1029/2010JD015401, _eprint: https://onlinelibrary.wiley.com/doi/pdf/10.1029/2010JD015401, 2011a.
- Rigby, M., Manning, A. J., and Prinn, R. G.: Inversion of long-lived trace gas emissions using combined Eulerian and Lagrangian chemical transport models, Atmospheric Chemistry and Physics, 11, 9887–9898, https://doi.org/10.5194/acp-11-9887-2011, 2011b.

885

- Rigby, M., Prinn, R. G., O'Doherty, S., Montzka, S. A., McCulloch, A., Harth, C. M., Mühle, J., Salameh, P. K., Weiss, R. F., Young, D., Simmonds, P. G., Hall, B. D., Dutton, G. S., Nance, D., Mondeel, D. J., Elkins, J. W., Krummel, P. B., Steele, L. P., and Fraser, P. J.: Re-evaluation of the lifetimes of the major CFCs and CH₃CCl₃ using atmospheric trends, Atmospheric Chemistry and Physics, 13, 2691–2702, https://doi.org/10.5194/acp-13-2691-2013, publisher: Copernicus GmbH, 2013.
- Rigby, M., Prinn, R. G., O'Doherty, S., Miller, B. R., Ivy, D., Mühle, J., Harth, C. M., Salameh, P. K., Arnold, T., Weiss, R. F., Krummel, P. B., Steele, L. P., Fraser, P. J., Young, D., and Simmonds, P. G.: Recent and future trends in synthetic greenhouse gas radiative forcing, Geophysical Research Letters, 41, 2623–2630, https://doi.org/10.1002/2013GL059099, _eprint: https://agupubs.onlinelibrary.wiley.com/doi/pdf/10.1002/2013GL059099, 2014.
- Rigby, M., Montzka, S. A., Prinn, R. G., White, J. W. C., Young, D., O'Doherty, S., Lunt, M. F., Ganesan, A. L., Manning, A. J., Simmonds, P. G., Salameh, P. K., Harth, C. M., Mühle, J., Weiss, R. F., Fraser, P. J., Steele, L. P., Krummel, P. B., McCulloch, A., and Park, S.: Role of atmospheric oxidation in recent methane growth, Proceedings of the National Academy of Sciences, 114, 5373–5377, https://doi.org/10.1073/pnas.1616426114, 2017.
- Rigby, M., Park, S., Saito, T., Western, L. M., Redington, A. L., Fang, X., Henne, S., Manning, A. J., Prinn, R. G., Dutton, G. S., Fraser, P. J., Ganesan, A. L., Hall, B. D., Harth, C. M., Kim, J., Kim, K.-R., Krummel, P. B., Lee, T., Li, S., Liang, Q., Lunt, M. F., Montzka, S. A., Mühle, J., O'Doherty, S., Park, M.-K., Reimann, S., Salameh, P. K., Simmonds, P., Tunnicliffe, R. L., Weiss, R. F., Yokouchi, Y., and Young, D.: Increase in CFC-11 emissions from eastern China based on atmospheric observations, Nature, 569, 546–550, https://doi.org/10.1038/s41586-019-1193-4, 2019.
 - Ruppel, C. D. and Kessler, J. D.: The interaction of climate change and methane hydrates, Reviews of Geophysics, 55, 126–168, https://doi.org/10.1002/2016RG000534, _eprint: https://onlinelibrary.wiley.com/doi/pdf/10.1002/2016RG000534, 2017.
 - Saikawa, E., Rigby, M., Prinn, R. G., Montzka, S. A., Miller, B. R., Kuijpers, L. J. M., Fraser, P. J. B., Vollmer, M. K., Saito, T., Yokouchi, Y., Harth, C. M., Mühle, J., Weiss, R. F., Salameh, P. K., Kim, J., Li, S., Park, S., Kim, K.-R., Young, D., O'Doherty, S., Simmonds, P. G., McCulloch, A., Krummel, P. B., Steele, L. P., Lunder, C., Hermansen, O., Maione, M., Arduini, J., Yao, B., Zhou, L. X., Wang, H. J., Elkins, J. W., and Hall, B.: Global and regional emission estimates for HCFC-22, Atmospheric Chemistry and Physics, 12, 10 033–10 050, https://doi.org/10.5194/acp-12-10033-2012, 2012.
 - Saikawa, E., Prinn, R. G., Dlugokencky, E., Ishijima, K., Dutton, G. S., Hall, B. D., Langenfelds, R., Tohjima, Y., Machida, T., Manizza, M., Rigby, M., O'Doherty, S., Patra, P. K., Harth, C. M., Weiss, R. F., Krummel, P. B., van der Schoot, M., Fraser, P. J., Steele, L. P., Aoki, S.,

- Nakazawa, T., and Elkins, J. W.: Global and regional emissions estimates for N₂O, Atmospheric Chemistry and Physics, 14, 4617–4641, https://doi.org/10.5194/acp-14-4617-2014, publisher: Copernicus GmbH, 2014.
- Saunois, M., Martinez, A., Poulter, B., Zhang, Z., Raymond, P., Regnier, P., Canadell, J. G., Jackson, R. B., Patra, P. K., Bousquet, P., Ciais, P., Dlugokencky, E. J., Lan, X., Allen, G. H., Bastviken, D., Beerling, D. J., Belikov, D. A., Blake, D. R., Castaldi, S., Crippa, M., Deemer, B. R., Dennison, F., Etiope, G., Gedney, N., Höglund-Isaksson, L., Holgerson, M. A., Hopcroft, P. O., Hugelius, G., Ito, A., Jain, A. K., Janardanan, R., Johnson, M. S., Kleinen, T., Krummel, P., Lauerwald, R., Li, T., Liu, X., McDonald, K. C., Melton, J. R., Mühle, J., Müller, J., Murguia-Flores, F., Niwa, Y., Noce, S., Pan, S., Parker, R. J., Peng, C., Ramonet, M., Riley, W. J., Rocher-Ros, G., Rosentreter, J. A.,
 Sasakawa, M., Segers, A., Smith, S. J., Stanley, E. H., Thanwerdas, J., Tian, H., Tsuruta, A., Tubiello, F. N., Weber, T. S., Van Der Werf, G., Worthy, D. E., Xi, Y., Yoshida, Y., Zhang, W., Zheng, B., Zhu, O., Zhu, O., and Zhuang, O.: Global Methane Budget 2000–2020.

https://doi.org/10.5194/essd-2024-115, 2024.

- Saunois, M., Martinez, A., Poulter, B., Zhang, Z., Raymond, P. A., Regnier, P., Canadell, J. G., Jackson, R. B., Patra, P. K., Bousquet, P., Ciais, P., Dlugokencky, E. J., Lan, X., Allen, G. H., Bastviken, D., Beerling, D. J., Belikov, D. A., Blake, D. R., Castaldi, S., Crippa,
- M., Deemer, B. R., Dennison, F., Etiope, G., Gedney, N., Höglund-Isaksson, L., Holgerson, M. A., Hopcroft, P. O., Hugelius, G., Ito, A., Jain, A. K., Janardanan, R., Johnson, M. S., Kleinen, T., Krummel, P. B., Lauerwald, R., Li, T., Liu, X., McDonald, K. C., Melton, J. R., Mühle, J., Müller, J., Murguia-Flores, F., Niwa, Y., Noce, S., Pan, S., Parker, R. J., Peng, C., Ramonet, M., Riley, W. J., Rocher-Ros, G., Rosentreter, J. A., Sasakawa, M., Segers, A., Smith, S. J., Stanley, E. H., Thanwerdas, J., Tian, H., Tsuruta, A., Tubiello, F. N., Weber, T. S., Van Der Werf, G. R., Worthy, D. E. J., Xi, Y., Yoshida, Y., Zhang, W., Zheng, B., Zhu, Q., Zhu, Q., and Zhuang, Q.: Global Methane
 Budget 2000–2020, Earth System Science Data, 17, 1873–1958, https://doi.org/10.5194/essd-17-1873-2025, 2025.
 - Schaefer, H., Fletcher, S. E. M., Veidt, C., Lassey, K. R., Brailsford, G. W., Bromley, T. M., Dlugokencky, E. J., Michel, S. E., Miller, J. B., Levin, I., Lowe, D. C., Martin, R. J., Vaughn, B. H., and White, J. W. C.: A 21st-century shift from fossil-fuel to biogenic methane emissions indicated by ¹³CH₄, Science, 352, 80–84, https://doi.org/10.1126/science.aad2705, 2016.
- Schoenenberger, F., Vollmer, M. K., Rigby, M., Hill, M., Fraser, P. J., Krummel, P. B., Langenfelds, R. L., Rhee, T. S., Peter, T., and Reimann,

 S.: First observations, trends, and emissions of HCFC-31 (CH₂ClF)in the global atmosphere, Geophysical Research Letters, 42, 7817–7824, https://doi.org/10.1002/2015GL064709, 2015.
 - Sherry, D., McCulloch, A., Liang, Q., Reimann, S., and Newman, P. A.: Current sources of carbon tetrachloride (CCl₄) in our atmosphere, Environmental Research Letters, 13, 024 004, https://doi.org/10.1088/1748-9326/aa9c87, 2018.
- Sherwen, T., Schmidt, J. A., Evans, M. J., Carpenter, L. J., Großmann, K., Eastham, S. D., Jacob, D. J., Dix, B., Koenig, T. K., Sinreich, R., Ortega, I., Volkamer, R., Saiz-Lopez, A., Prados-Roman, C., Mahajan, A. S., and Ordóñez, C.: Global impacts of tropospheric halogens (Cl, Br, I) on oxidants and composition in GEOS-Chem, Atmospheric Chemistry and Physics, 16, 12 239–12 271, https://doi.org/10.5194/acp-16-12239-2016, publisher: Copernicus GmbH, 2016.
 - Shine, K. P. and Myhre, G.: The Spectral Nature of Stratospheric Temperature Adjustment and its Application to Halocarbon Radiative Forcing, Journal of Advances in Modeling Earth Systems, 12, e2019MS001951, https://doi.org/10.1029/2019MS001951, _eprint: https://onlinelibrary.wiley.com/doi/pdf/10.1029/2019MS001951, 2020.
 - Simmonds, P. G., O'Doherty, S., Nickless, G., Sturrock, G. A., Swaby, R., Knight, P., Ricketts, J., Woffendin, G., and Smith, R.: Automated Gas Chromatograph/Mass Spectrometer for Routine Atmospheric Field Measurements of the CFC Replacement Compounds, the Hydrofluorocarbons and Hydrochlorofluorocarbons, Analytical Chemistry, 67, 717–723, https://doi.org/10.1021/ac00100a005, 1995.
- Simmonds, P. G., Manning, A. J., Cunnold, D. M., McCulloch, A., O'Doherty, S., Derwent, R. G., Krummel, P. B., Fraser, P. J., Dunse, B., Porter, L. W., Wang, R. H. J., Greally, B. R., Miller, B. R., Salameh, P., Weiss, R. F., and Prinn, R. G.: Global trends, seasonal

- cycles, and European emissions of dichloromethane, trichloroethene, and tetrachloroethene from the AGAGE observations at Mace Head, Ireland, and Cape Grim, Tasmania, Journal of Geophysical Research: Atmospheres, 111, https://doi.org/10.1029/2006JD007082, _eprint: https://onlinelibrary.wiley.com/doi/pdf/10.1029/2006JD007082, 2006.
- Simmonds, P. G., Rigby, M., Manning, A. J., Lunt, M. F., O'Doherty, S., McCulloch, A., Fraser, P. J., Henne, S., Vollmer, M. K., Mühle, J., Weiss, R. F., Salameh, P. K., Young, D., Reimann, S., Wenger, A., Arnold, T., Harth, C. M., Krummel, P. B., Steele, L. P., Dunse, B. L., Miller, B. R., Lunder, C. R., Hermansen, O., Schmidbauer, N., Saito, T., Yokouchi, Y., Park, S., Li, S., Yao, B., Zhou, L. X., Arduini, J., Maione, M., Wang, R. H. J., Ivy, D., and Prinn, R. G.: Global and regional emissions estimates of 1,1-difluoroethane (HFC-152a, CH₃CHF₂) from in situ and air archive observations, Atmospheric Chemistry and Physics, 16, 365–382, https://doi.org/10.5194/acp-16-365-2016, publisher: Copernicus GmbH, 2016.
- 940 Simmonds, P. G., Rigby, M., McCulloch, A., O'Doherty, S., Young, D., Mühle, J., Krummel, P. B., Steele, P., Fraser, P. J., Manning, A. J., Weiss, R. F., Salameh, P. K., Harth, C. M., Wang, R. H. J., and Prinn, R. G.: Changing trends and emissions of hydrochlorofluorocarbons (HCFCs) and their hydrofluorocarbon (HFCs) replacements, Atmospheric Chemistry and Physics, 17, 4641–4655, https://doi.org/10.5194/acp-17-4641-2017, 2017.
- Simmonds, P. G., Rigby, M., McCulloch, A., Vollmer, M. K., Henne, S., Mühle, J., O'Doherty, S., Manning, A. J., Krummel, P. B., Fraser, P. J., Young, D., Weiss, R. F., Salameh, P. K., Harth, C. M., Reimann, S., Trudinger, C. M., Steele, L. P., Wang, R. H. J., Ivy, D. J., Prinn, R. G., Mitrevski, B., and Etheridge, D. M.: Recent increases in the atmospheric growth rate and emissions of HFC-23 (CHF₃) and the link to HCFC-22 (CHClF₂) production, Atmospheric Chemistry and Physics, 18, 4153–4169, https://doi.org/10.5194/acp-18-4153-2018, publisher: Copernicus GmbH, 2018.
- Simmonds, P. G., Rigby, M., Manning, A. J., Park, S., Stanley, K. M., McCulloch, A., Henne, S., Graziosi, F., Maione, M., Arduini, J., Park, S., Vollmer, M. K., Mühle, J., O'Doherty, S., Young, D., Krummel, P. B., Fraser, P. J., Weiss, R. F., Salameh, P. K., Harth, C. M., Park, M.-K., Park, H., Arnold, T., Rennick, C., Steele, L. P., Mitrevski, B., Wang, R. H. J., and Prinn, R. G.: The increasing atmospheric burden of the greenhouse gas sulfur hexafluoride (SF₆), Atmospheric Chemistry and Physics, 20, 7271–7290, https://doi.org/10.5194/acp-20-7271-2020, publisher: Copernicus GmbH, 2020.
- Spivakovsky, C. M., Logan, J. A., Montzka, S. A., Balkanski, Y. J., Foreman-Fowler, M., Jones, D. B. A., Horowitz, L. W., Fusco, A. C.,

 Brenninkmeijer, C. a. M., Prather, M. J., Wofsy, S. C., and McElroy, M. B.: Three-dimensional climatological distribution of tropospheric OH: Update and evaluation, Journal of Geophysical Research: Atmospheres, 105, 8931–8980, https://doi.org/10.1029/1999JD901006, _eprint: https://onlinelibrary.wiley.com/doi/pdf/10.1029/1999JD901006, 2000.
 - Stanley, K. M., Say, D., Mühle, J., Harth, C. M., Krummel, P. B., Young, D., O'Doherty, S. J., Salameh, P. K., Simmonds, P. G., Weiss, R. F., Prinn, R. G., Fraser, P. J., and Rigby, M.: Increase in global emissions of HFC-23 despite near-total expected reductions, Nature Communications, 11, 1–6, https://doi.org/10.1038/s41467-019-13899-4, number: 1 Publisher: Nature Publishing Group, 2020.

- Stell, A. C., Western, L. M., Sherwen, T., and Rigby, M.: Atmospheric-methane source and sink sensitivity analysis using Gaussian process emulation, Atmospheric Chemistry and Physics, 21, 1717–1736, https://doi.org/10.5194/acp-21-1717-2021, publisher: Copernicus GmbH, 2021.
- Stell, A. C., Bertolacci, M., Zammit-Mangion, A., Rigby, M., Fraser, P. J., Harth, C. M., Krummel, P. B., Lan, X., Manizza, M., Mühle, J.,
 O'Doherty, S., Prinn, R. G., Weiss, R. F., Young, D., and Ganesan, A. L.: Modelling the growth of atmospheric nitrous oxide using a global hierarchical inversion, Atmospheric Chemistry and Physics, 22, 12945–12960, https://doi.org/10.5194/acp-22-12945-2022, publisher: Copernicus GmbH, 2022.

- Thompson, R. L., Nisbet, E. G., Pisso, I., Stohl, A., Blake, D., Dlugokencky, E. J., Helmig, D., and White, J. W. C.: Variability in Atmospheric Methane From Fossil Fuel and Microbial Sources Over the Last Three Decades, Geophysical Research Letters, 45, https://doi.org/10.1029/2018GL078127, 2018.
 - Thompson, R. L., Montzka, S. A., Vollmer, M. K., Arduini, J., Crotwell, M., Krummel, P. B., Lunder, C., Mühle, J., O'Doherty, S., Prinn, R. G., Reimann, S., Vimont, I., Wang, H., Weiss, R. F., and Young, D.: Estimation of the atmospheric hydroxyl radical oxidative capacity using multiple hydrofluorocarbons (HFCs), Atmospheric Chemistry and Physics, 24, 1415–1427, https://doi.org/10.5194/acp-24-1415-2024, publisher: Copernicus GmbH, 2024.
- Tian, H., Pan, N., Thompson, R. L., Canadell, J. G., Suntharalingam, P., Regnier, P., Davidson, E. A., Prather, M., Ciais, P., Muntean, M., Pan, S., Winiwarter, W., Zaehle, S., Zhou, F., Jackson, R. B., Bange, H. W., Berthet, S., Bian, Z., Bianchi, D., Bouwman, A. F., Buitenhuis, E. T., Dutton, G., Hu, M., Ito, A., Jain, A. K., Jeltsch-Thömmes, A., Joos, F., Kou-Giesbrecht, S., Krummel, P. B., Lan, X., Landolfi, A., Lauerwald, R., Li, Y., Lu, C., Maavara, T., Manizza, M., Millet, D. B., Mühle, J., Patra, P. K., Peters, G. P., Qin, X., Raymond, P., Resplandy, L., Rosentreter, J. A., Shi, H., Sun, Q., Tonina, D., Tubiello, F. N., Van Der Werf, G. R., Vuichard, N., Wang, J., Wells, K. C.,
 Western, L. M., Wilson, C., Yang, J., Yao, Y., You, Y., and Zhu, Q.: Global nitrous oxide budget (1980–2020), Earth System Science Data,

16, 2543-2604, https://doi.org/10.5194/essd-16-2543-2024, 2024.

- Trudinger, C. M., Etheridge, D. M., Sturrock, G. A., Fraser, P. J., Krummel, P. B., and McCulloch, A.: Atmospheric histories of halocarbons from analysis of Antarctic firn air: Methyl bromide, methyl chloride, chloroform, and dichloromethane, Journal of Geophysical Research: Atmospheres, 109, 2004JD004 932, https://doi.org/10.1029/2004JD004932, 2004.
- Trudinger, C. M., Fraser, P. J., Etheridge, D. M., Sturges, W. T., Vollmer, M. K., Rigby, M., Martinerie, P., Mühle, J., Worton, D. R., Krummel, P. B., Steele, L. P., Miller, B. R., Laube, J., Mani, F. S., Rayner, P. J., Harth, C. M., Witrant, E., Blunier, T., Schwander, J., O'Doherty, S., and Battle, M.: Atmospheric abundance and global emissions of perfluorocarbons CF₄, C₂F₆ and C₃F₈ since 1800 inferred from ice core, firn, air archive and in situ measurements, Atmospheric Chemistry and Physics, 16, 11733–11754, https://doi.org/10.5194/acp-16-11733-2016, publisher: Copernicus GmbH, 2016.
- Turner, A. J., Frankenberg, C., Wennberg, P. O., and Jacob, D. J.: Ambiguity in the causes for decadal trends in atmospheric methane and hydroxyl, Proceedings of the National Academy of Sciences, 114, 5367–5372, https://doi.org/10.1073/pnas.1616020114, 2017.
 - van der Werf, G. R., Randerson, J. T., Giglio, L., van Leeuwen, T. T., Chen, Y., Rogers, B. M., Mu, M., van Marle, M. J. E., Morton, D. C., Collatz, G. J., Yokelson, R. J., and Kasibhatla, P. S.: Global fire emissions estimates during 1997–2016, Earth System Science Data, 9, 697–720, https://doi.org/10.5194/essd-9-697-2017, 2017.
- Velders, G. J. M., Daniel, J. S., Montzka, S. A., Vimont, I., Rigby, M., Krummel, P. B., Muhle, J., O'Doherty, S., Prinn, R. G., Weiss, R. F., and Young, D.: Projections of hydrofluorocarbon (HFC) emissions and the resulting global warming based on recent trends in observed abundances and current policies, Atmospheric Chemistry and Physics, 22, 6087–6101, https://doi.org/10.5194/acp-22-6087-2022, publisher: Copernicus GmbH, 2022.
- Vollmer, M. K., Miller, B. R., Rigby, M., Reimann, S., Mühle, J., Krummel, P. B., O'Doherty, S., Kim, J., Rhee, T. S., Weiss, R. F., Fraser, P. J.,
 Simmonds, P. G., Salameh, P. K., Harth, C. M., Wang, R. H. J., Steele, L. P., Young, D., Lunder, C. R., Hermansen, O., Ivy, D., Arnold, T.,
 Schmidbauer, N., Kim, K.-R., Greally, B. R., Hill, M., Leist, M., Wenger, A., and Prinn, R. G.: Atmospheric histories and global emissions of the anthropogenic hydrofluorocarbons HFC-365mfc, HFC-245fa, HFC-227ea, and HFC-236fa, Journal of Geophysical Research: Atmospheres, 116, https://doi.org/10.1029/2010JD015309, _eprint: https://onlinelibrary.wiley.com/doi/pdf/10.1029/2010JD015309, 2011.

- Vollmer, M. K., Reimann, S., Hill, M., and Brunner, D.: First Observations of the Fourth Generation Synthetic Halocarbons

 HFC-1234yf, HFC-1234ze(E), and HCFC-1233zd(E) in the Atmosphere, Environmental Science & Technology, 49, 2703–2708,
 https://doi.org/10.1021/es505123x, publisher: American Chemical Society, 2015a.
 - Vollmer, M. K., Rhee, T. S., Rigby, M., Hofstetter, D., Hill, M., Schoenenberger, F., and Reimann, S.: Modern inhalation anesthetics: Potent greenhouse gases in the global atmosphere, Geophysical Research Letters, 42, 1606–1611, https://doi.org/10.1002/2014GL062785, _eprint: https://onlinelibrary.wiley.com/doi/pdf/10.1002/2014GL062785, 2015b.
- Vollmer, M. K., Rigby, M., Laube, J. C., Henne, S., Rhee, T. S., Gooch, L. J., Wenger, A., Young, D., Steele, L. P., Langenfelds, R. L., Brenninkmeijer, C. A. M., Wang, J.-L., Ou-Yang, C.-F., Wyss, S. A., Hill, M., Oram, D. E., Krummel, P. B., Schoenenberger, F., Zellweger, C., Fraser, P. J., Sturges, W. T., O'Doherty, S., and Reimann, S.: Abrupt reversal in emissions and atmospheric abundance of HCFC-133a (CF₃CH₂Cl), Geophysical Research Letters, 42, 8702–8710, https://doi.org/10.1002/2015GL065846, _eprint: https://onlinelibrary.wiley.com/doi/pdf/10.1002/2015GL065846, 2015c.
- Vollmer, M. K., Mühle, J., Trudinger, C. M., Rigby, M., Montzka, S. A., Harth, C. M., Miller, B. R., Henne, S., Krummel, P. B., Hall, B. D., Young, D., Kim, J., Arduini, J., Wenger, A., Yao, B., Reimann, S., O'Doherty, S., Maione, M., Etheridge, D. M., Li, S., Verdonik, D. P., Park, S., Dutton, G., Steele, L. P., Lunder, C. R., Rhee, T. S., Hermansen, O., Schmidbauer, N., Wang, R. H. J., Hill, M., Salameh, P. K., Langenfelds, R. L., Zhou, L., Blunier, T., Schwander, J., Elkins, J. W., Butler, J. H., Simmonds, P. G., Weiss, R. F., Prinn, R. G., and Fraser, P. J.: Atmospheric histories and global emissions of halons H-1211 (CBrClF₂), H-1301 (CBrF₃), and H-2402
- 1020 (CBrF₂CBrF₂), Journal of Geophysical Research: Atmospheres, 121, 3663–3686, https://doi.org/https://doi.org/10.1002/2015JD024488, _eprint: https://agupubs.onlinelibrary.wiley.com/doi/pdf/10.1002/2015JD024488, 2016.
 - Vollmer, M. K., Young, D., Trudinger, C. M., Mühle, J., Henne, S., Rigby, M., Park, S., Li, S., Guillevic, M., Mitrevski, B., Harth, C. M., Miller, B. R., Reimann, S., Yao, B., Steele, L. P., Wyss, S. A., Lunder, C. R., Arduini, J., McCulloch, A., Wu, S., Rhee, T. S., Wang, R. H. J., Salameh, P. K., Hermansen, O., Hill, M., Langenfelds, R. L., Ivy, D., O'Doherty, S., Krummel, P. B., Maione, M., Etheridge, D. M., Zhou,
- L., Fraser, P. J., Prinn, R. G., Weiss, R. F., and Simmonds, P. G.: Atmospheric histories and emissions of chlorofluorocarbons CFC-13 (CClF₃), ΣCFC-114 (C₂Cl₂F₄), and CFC-115 (C₂ClF₅), Atmospheric Chemistry and Physics, 18, 979–1002, https://doi.org/10.5194/acp-18-979-2018, publisher: Copernicus GmbH, 2018.

- Vollmer, M. K., Bernard, F., Mitrevski, B., Steele, L. P., Trudinger, C. M., Reimann, S., Langenfelds, R. L., Krummel, P. B., Fraser, P. J., Etheridge, D. M., Curran, M. A. J., and Burkholder, J. B.: Abundances, emissions, and loss processes of the long-lived and potent greenhouse gas octafluorooxolane (octafluorotetrahydrofuran, *c*-C₄F₈O) in the atmosphere, Atmospheric Chemistry and Physics, 19, 3481–3492, https://doi.org/10.5194/acp-19-3481-2019, 2019.
- Vollmer, M. K., Mühle, J., Henne, S., Young, D., Rigby, M., Mitrevski, B., Park, S., Lunder, C. R., Rhee, T. S., Harth, C. M., Hill, M., Langenfelds, R. L., Guillevic, M., Schlauri, P. M., Hermansen, O., Arduini, J., Wang, R. H. J., Salameh, P. K., Maione, M., Krummel, P. B., Reimann, S., O'Doherty, S., Simmonds, P. G., Fraser, P. J., Prinn, R. G., Weiss, R. F., and Steele, L. P.: Unexpected nascent atmospheric emissions of three ozone-depleting hydrochlorofluorocarbons, Proceedings of the National Academy of Sciences, 118, e2010914118,
- emissions of three ozone-depleting hydrochlorofluorocarbons, Proceedings of the National Academy of Sciences, 118, e2010914118 https://doi.org/10.1073/pnas.2010914118, 2021.
 - Wang, P., Scott, J. R., Solomon, S., Marshall, J., Babbin, A. R., Lickley, M., Thompson, D. W. J., DeVries, T., Liang, Q., and Prinn, R. G.: On the effects of the ocean on atmospheric CFC-11 lifetimes and emissions, Proceedings of the National Academy of Sciences, 118, e2021528118, https://doi.org/10.1073/pnas.2021528118, 2021.
- 1040 Weiss, R. F., Mühle, J., Salameh, P. K., and Harth, C. M.: Nitrogen trifluoride in the global atmosphere, Geophysical Research Letters, 35, https://doi.org/10.1029/2008GL035913, _eprint: https://onlinelibrary.wiley.com/doi/pdf/10.1029/2008GL035913, 2008.

- Western, L. M., Redington, A. L., Manning, A. J., Trudinger, C. M., Hu, L., Henne, S., Fang, X., Kuijpers, L. J. M., Theodoridi, C., Godwin, D. S., Arduini, J., Dunse, B., Engel, A., Fraser, P. J., Harth, C. M., Krummel, P. B., Maione, M., Mühle, J., O'Doherty, S., Park, H., Park, S., Reimann, S., Salameh, P. K., Say, D., Schmidt, R., Schuck, T., Siso, C., Stanley, K. M., Vimont, I., Vollmer, M. K., Young, D., Prinn,
- R. G., Weiss, R. F., Montzka, S. A., and Rigby, M.: A renewed rise in global HCFC-141b emissions between 2017–2021, Atmospheric Chemistry and Physics, 22, 9601–9616, https://doi.org/10.5194/acp-22-9601-2022, publisher: Copernicus GmbH, 2022.

1070

- Western, L. M., Vollmer, M. K., Krummel, P. B., Adcock, K. E., Crotwell, M., Fraser, P. J., Harth, C. M., Langenfelds, R. L., Montzka, S. A., Mühle, J., O'Doherty, S., Oram, D. E., Reimann, S., Rigby, M., Vimont, I., Weiss, R. F., Young, D., and Laube, J. C.: Global increase of ozone-depleting chlorofluorocarbons from 2010 to 2020, Nature Geoscience, 16, 309–313, https://doi.org/10.1038/s41561-023-01147-w, 2023.
- Western, L. M., Bachman, S. D., Montzka, S. A., and Rigby, M.: MALTA: A Zonally Averaged Global Atmospheric Transport Model for Long-Lived Trace Gases, Journal of Advances in Modeling Earth Systems, 16, e2023MS003 909, https://doi.org/10.1029/2023MS003909, 2024a.
- Western, L. M., Daniel, J. S., Vollmer, M. K., Clingan, S., Crotwell, M., Fraser, P. J., Ganesan, A. L., Hall, B., Harth, C. M., Krummel, P. B.,
 Mühle, J., O'Doherty, S., Salameh, P. K., Stanley, K. M., Reimann, S., Vimont, I., Young, D., Rigby, M., Weiss, R. F., Prinn, R. G., and Montzka, S. A.: A decrease in radiative forcing and equivalent effective chlorine from hydrochlorofluorocarbons, Nature Climate Change, https://doi.org/10.1038/s41558-024-02038-7, 2024b.
 - Western, L. M., Rigby, M., Mühle, J., Krummel, P. B., Lunder, C. R., O'Doherty, S., Reimann, S., Vollmer, M. K., Adam, B., Fraser, P. J., Ganesan, A. L., Harth, C. M., Hermansen, O., Kim, J., Langenfelds, R. L., Loh, Z. M., Mitrevski, B., Pitt, J. R., Salameh, P. K., Schmidt,
- R., Stanley, K., Stavert, A. R., Wang, H.-J. R., Young, D., Weiss, R. F., and Prinn, R. G.: Global Emissions and Abundances of Chemically and Radiatively Important Trace Gases from the AGAGE Network, https://doi.org/10.5281/zenodo.15586140, 2025.
 - Worden, J. R., Bloom, A. A., Pandey, S., Jiang, Z., Worden, H. M., Walker, T. W., Houweling, S., and Röckmann, T.: Reduced biomass burning emissions reconcile conflicting estimates of the post-2006 atmospheric methane budget, Nature Communications, 8, https://doi.org/10.1038/s41467-017-02246-0, 2017.
- 1065 Xiao, X.: Optimal Estimation of the Surface Fluxes of Chloromethanes Using a 3-D Global Atmospheric Chemical Transport Model, PhD Thesis, Massachusetts Institute of Technology, https://dspace.mit.edu/bitstream/handle/1721.1/45603/318453304-MIT.pdf?sequence=2&isAllowed=y#page=133.83, 2008.
 - Yan, X., Akiyama, H., Yagi, K., and Akimoto, H.: Global estimations of the inventory and mitigation potential of methane emissions from rice cultivation conducted using the 2006 Intergovernmental Panel on Climate Change Guidelines: Methane Emission from Global Rice Fields, Global Biogeochemical Cycles, 23, https://doi.org/10.1029/2008GB003299, 2009.
 - Yang, W. and Zurbenko, I.: Kolmogorov–Zurbenko filters, WIREs Computational Statistics, 2, 340–351, https://doi.org/10.1002/wics.71, _eprint: https://onlinelibrary.wiley.com/doi/pdf/10.1002/wics.71, 2010.
 - Yvon-Lewis, S. A. and Butler, J. H.: The potential effect of oceanic biological degradation on the lifetime of atmospheric CH₃Br, Geophysical Research Letters, 24, 1227–1230, https://doi.org/10.1029/97GL01090, _eprint: https://onlinelibrary.wiley.com/doi/pdf/10.1029/97GL01090, 1997.
 - Yvon-Lewis, S. A. and Butler, J. H.: Effect of oceanic uptake on atmospheric lifetimes of selected trace gases, Journal of Geophysical Research: Atmospheres, 107, ACH 1–1–ACH 1–9, https://doi.org/10.1029/2001JD001267, _eprint: https://onlinelibrary.wiley.com/doi/pdf/10.1029/2001JD001267, 2002.

Zhang, Z., Poulter, B., Feldman, A. F., Ying, Q., Ciais, P., Peng, S., and Li, X.: Recent intensification of wetland methane feedback, Nature Climate Change, 13, 430–433, https://doi.org/10.1038/s41558-023-01629-0, publisher: Nature Publishing Group, 2023.